Detection of Local Steroidogenic Enzyme Gene Expression in Brown Anoles

Ada Spahija

April 27, 2018

Advisor: Dr. Bobby Fokidis

In partial fulfillment of the Rollins College Honors Degree Program
as well as the Requirements for
Honors in the Major in Biochemistry and Molecular Biology

Abstract

The endocrine system in vertebrates responds to stress by releasing steroid hormones, mainly glucocorticoids (GC), which increase blood glucose levels to supply key organs and muscles with energy needed for survival. Steroid hormones are synthesized via an enzymatic pathway that converts cholesterol into either GCs, androgens, or estrogens in a step-wise manner. The adrenal cortex is known to produce GCs, but evidence suggests that individual organs can also produce steroid hormones *de novo* in response to stress. This study aims to quantify gene expression of four steroidogenic enzymes, encoded by CYP19A1, CYP17A1, StAR, and HSD17ß3 genes, via qRT-PCR to determine if the stress of fasting in *Anolis sagrei* (brown anole) increases local steroidogenesis in comparison to fed organisms. RNA extraction protocol as well as CYP17A1 and StAR primer concentrations for qRT-PCR were optimized, paving the way for successful quantification of steroidogenic enzyme gene expression in the brown anole. In the future, this quantification could establish the variability of expression of these genes, not only amongst organs, but also between stressed and non-stressed organisms.

Introduction

Animal physiology is greatly affected by stress, which can occur as a result of a variety of events that pose a potential challenge or threat to an animal's wellbeing, such as attack by a predator or metabolic distress caused by food shortage. When experiencing stress, the endocrine system in vertebrates functions to promote survival by increasing the animal's heart rate, breathing, mental alertness, and energy availability, so that it is prepared to face the stressor (Sapolsky et al., 2000). In the first "rapid" phase of this stress response, the catecholamine neurotransmitters, epinephrine and norepinephrine, named for their common chemical structure in which a benzene ring has two hydroxyl side groups and one side chain amine, are released from the adrenal medulla

to quickly increase blood flow via blood vessel dilation, increased heart rate, and increased breathing rate (Charmandari et al., 2005). This response provides the essential oxygen and nutrients to tissues that are necessary for immediate survival, such as skeletal muscle that is needed to evade a predator or hunt for food. The second "slow" phase initiates three to five minutes later and is characterized by the secretion of steroid hormones from the adrenal cortex into the blood (Charmandari et al., 2005). Most prominent of these are glucocorticoids (GCs), with corticosterone (CORT) being the primary GC in reptiles, birds, and small mammals, and cortisol being secreted in humans (Sapolsky et al., 2000).

The release of GCs into the blood stream permits them to bind to receptors in various tissues and ultimately results in physiological responses throughout the body that aid the organism in surviving the stress. This occurs through the glucocorticoid's impact on metabolism and behavior, which are both necessary in providing the energy and psychological drive for the organism's response. CORT decreases plasma testosterone levels, aiding in conserving the bodies energy by reducing reproductive function and reducing aggressive behavior (Tokarz, 1987). Metabolically, high levels of GCs increase the production and circulation of glucose by inhibiting glucose uptake in gastrointestinal tissues and mobilizing glucose in the circulatory system to make it accessible to skeletal and cardiac muscles (Leung and Munck, 1975). This role of GCs makes their release important to animals during energetic challenges, such as fasting, by providing energy for the animal to face the stressor via increased glucose availability.

The nature of stress, whether it is acute or chronic, can also affect the body's hormonal and physiological response. During acute stress, which is caused by an immediate temporary threat, the release of GCs causes reactive responses to immediately prepare for the stressor. For example, studies in male rodents that have experienced food restriction have shown that increased GCs cause

decreased testosterone, which immediately aids in energy conservation in the organism by reducing energy usage for reproductive activities (De Boer et al., 1989). During chronic stress, in which the stressor is either prolonged or reoccurring, the reactive responses can be enhanced by hypersecretion of GCs (Jankord and Herman, 2009). However, chronic stress can also cause a decrease in GCs and overall steroidogenic activity (De Boer et al., 1989). This counter-intuitive response may be due to negative regulation of GCs that inhibits them from becoming hyperactive in the body for prolonged periods, in order to prevent adverse effects from the stress response over time, such as chronic high blood pressure and high blood glucose.

Corticosterone in Stress Response

Glucocorticoids that are released in the event of a stressor are regulated in numerous ways, including various hormone/receptor interactions, in order to control their widespread effects on the body (de Kloet et al., 2009). The limbic system, the part of the midbrain that integrates stressful stimuli to generate a response, first signals to neurons in the hypothalamus to produce corticotrophin releasing hormone (CRH) and other small-peptide neurotransmitters in the event of a stressor (Herman et al., 2005). These molecules facilitate the neuroendocrine response that initiates the hypothalamic-pituitary-adrenal (HPA) axis, a hormonal pathway that ultimately leads to the production of CORT. This pathway includes negative feedback regulation of the entire stress response, in which excess CORT targets the limbic system and stops it from signaling for more CORT production (de Kloet et al., 2009).

Glucocorticoids function to drive the body's stress response in a process that can be divided into two distinct stages. During the initial stress response, CORT prepares the body's defense through permissive actions, in which it regulates other hormones to allow them to exert their full function, such as increasing blood pressure and heart rate to prepare the muscles for

action by supplying them with oxygenated and nutrient-rich blood (Sapolsky et al., 2000). CORT mediates these stress responses by permitting CRH, which is produced prior to CORT, to signal sympathetic nervous system activation that increases cardiovascular and respiratory actions. In the secondary response, in which circulating CORT levels continue to rise, the actions of the GC become suppressive to prevent the body's reaction from being too intense and causing possible harm to the organism (Munck et al., 1984). For example, the first wave of the stress response serves to activate the immune system by increasing the growth of B cells and lymphocytes (McGillis et al., 1989). In the second wave, GCs become immunosuppressive to prevent inflammation caused by the rapid proliferation of immune cells. While both of these stages are important to the overall stress response, the most well known role of GCs is their stimulatory effect, in which the effects of the first wave of hormones are enhanced over a prolonged period of time (Sapolsky et al., 2000).

The extended stress response increases blood glucose concentration by stimulating appetite, gluconeogenesis, and proteolysis. During energetic challenges, this enhanced stress response stimulated by CORT is essential to the survival of an animal. Presence of GCs stimulates glycogen lysis and gluconeogenesis via activation of hormones that initiate these processes, such as glucagon and catecholamines (Brindley and Rolland, 1989). GCs also mobilize lipids and amino acids via activation of lipid breakdown in fat cells, inhibition of protein synthesis in muscle cells, and after extended metabolic stress, breakdown of proteins in muscles (DeFronzo et al., 1980). All of these actions of GCs permissively activate the metabolic stress response by allowing metabolic hormones to have enhanced function. This is essential for chronic stress, such as fasting, because the actions of glucagon and catecholamines alone are short lived, but extended release of GCs enhances and prolongs their effects (Munck et al., 1984).

The two opposing actions of CORT, its initial amplification of the stress response and subsequent inhibition of the limbic system due to negative feedback, can be explained by the different CORT receptors in the hippocampus of the brain (McEwen et al., 1968). CORT binds to both mineralocorticoid (MR) and glucocorticoid receptors (GR), but the activation of each of these receptors has very different consequences. When bound to MR, CORT has an excitatory effect on the body's reaction to stress by activating the HPA axis and enhancing signals in the brain that increase alertness and alter behavior to help face the stressor (Joëls, 2009). CORT has a very high affinity for MR and thus this is the primary receptor that is used for basal level stress response. After initial stress is perceived, CORT binds to GRs, dampening the body's stress response in order to allow for recovery and adaptation (Morsink et al., 2006). This occurs via GR's ability to interact with transcription factors that repress transcription of genes that are involved in the initial stress response. This balance of the activating and inhibiting actions of CORT via MR and GR activation is crucial to maintaining homeostasis in the animal that is experiencing a stressful event.

Hypothalamic-Pituitary-Adrenal (HPA) Axis

Physical and metabolic stressors are first perceived in the brain and processed via the HPA axis, a hormonal cascade that induces adrenal steroidogenesis and ultimately leads to glucocorticoid secretion, which activates the stress response of multiple organ systems. The HPA axis initiates within the hypothalamus, the primary endocrine regulatory center of the brain (Figure 1). Neurons in the periventricular nucleus of the hypothalamus (PVN) produce the peptide corticotrophin-releasing factor (CRF) in response to signals from the brain or other organs to indicate stress (Jankord and Herman, 2008).

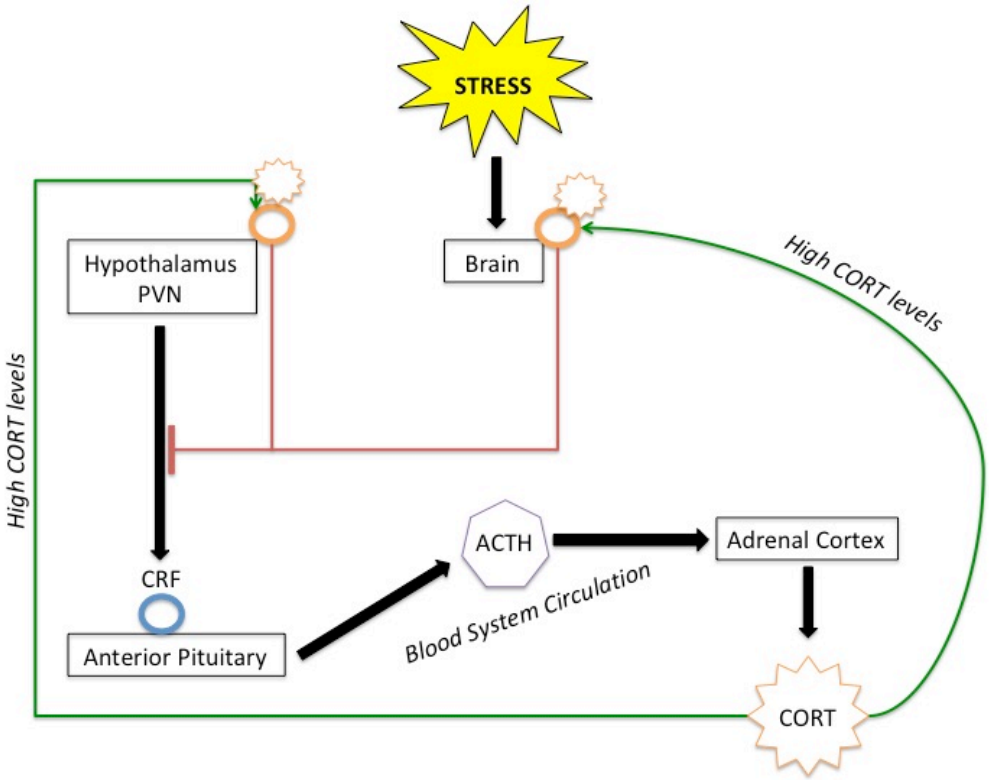

Figure 1. The HPA axis is a regulated hormonal pathway involving the hypothalamus, anterior pituitary, and adrenal cortex to ultimately lead to the production of glucocorticoids. Stress is perceived by the brain and the hypothalamus PVN releases corticotrophin-releasing factor (CRF), which binds to its receptor (shown as a blue circle) on the anterior pituitary, leading to the secretion of adrenocorticotropic hormone (ACTH) into the blood stream. ACTH binds to receptors in the adrenal cortex, causing production of CORT. A negative feedback loop leads to inhibition of the HPA axis (shown as red lines) when CORT binds to glucocorticoid receptors (shown as orange circles) in the hypothalamus and other areas of the brain.

CRF released from the PVN binds to CRF receptors, mainly CRFR1 in the anterior pituitary (Smith and Vale, 2006). Another CRF receptor, CRFR2, is expressed in peripheral tissues but does not bind CRF with as high affinity as CRFR1, and its role in the HPA axis remains unclear (Smith and Vale, 2006). In the anterior pituitary, CRF binds to its receptor and activates adenylate cyclase and cAMP pathways that lead to the release of adrenocorticotropic hormone (ACTH). Under normal conditions, CRF is secreted in a cyclic fashion with a higher overall amount secreted in the morning to promote alertness and the transition to active metabolism. Under acute stress, the amount and frequency of CRF secretion increase, leading to increased ACTH production

(Charmandari et al., 2005). CRF is also expressed in tissues outside of the central nervous system, such as the testis, gastrointestinal tract, and skin, providing plausibility for organ-specific HPA axes that could cause local steroid synthesis (Smith and Vale, 2006).

ACTH, produced in the pituitary, binds to the melanocortin type-two receptor (MC2-R) in parenchymal cells of the adrenal cortex, leading to the secretion of GCs from this part of the adrenal gland. This activation of steroidogenesis and secretion of glucocorticoids is accomplished by ACTH/MC2-R interaction promoting the conversion of cholesterol into pregnenolone, which is the first enzymatic step of GC synthesis (Charmandari et al., 2005).

The HPA axis is regulated primarily through negative feedback by glucocorticoids in the blood stream (Keller-Wood and Dallman, 1984). GC receptors are localized in areas of the brain that respond to stress and, when bound by GCs, regulate transcription of HPA axis factors that are required for the pathway to successfully produce GCs. GCs have a low binding affinity for GRs and thus only bind them when GC secretion is high, which occurs after stress (Smith and Vale, 2006). GRs can be found in the PVN at high levels and, when bound by GCs, reduce PVN activity, thus reducing ACTH secretion and HPA axis activity (Watts, 2005). The hippocampus also has a multitude of GRs, making it another site for negative regulation of the HPA axis (Jacobson and Sapolsky, 1991).

Feedback inhibition of the HPA axis is important so that animals do not experience negative effects of the GC-activated stress response, such as chronic high blood pressure or proteolysis that could result in cardiac and muscle damage. The hippocampus is one site of HPA regulation, as shown by increases in CORT secretion and HPA axis activity in mice with no hippocampal GRs (Feldmana and Weidenfeldb, 1999). The exact mechanisms that result in hippocampal regulation of the HPA axis have not been extensively studied, but a popular

hypothesis is that other biomolecules, particularly steroid hormones other than glucocorticoids, may have inhibitory roles that minimize the damage potentially caused by excess levels of GCs due to prolonged activity of the HPA axis (Jacobson and Sapolsky, 1991).

Interestingly, chronic exposure to stress can enhance HPA activity and prolong the body's stress response despite high levels of GCs that should initiate negative feedback, indicating that it is possible to evade this negative regulation (Jankord and Herman, 2009). This aspect of endocrinology remains unclear, but a possible mechanism for this inhibition evasion could include the role of arginine vasopressin (AVP), a peptide expressed in the PVN and released to regulate osmolarity (Smith and Vale, 2006). CRF release stimulates AVP secretion and the peptide binds to AVP receptors, causing release of ACTH to stimulate the HPA axis. The expression of AVP is increased in response to chronic stress, rather than being decreased in response to negative feedback, suggesting that PVN cells are unresponsive to the GC feedback loop (Sawchenko, 1987). It is hypothesized that AVP is essential in maintaining the reactive actions of the HPA axis during chronic stress by stimulating ACTH regardless of GC levels (Smith and Vale, 2006).

DHEA and Testosterone in Stress Response

While the release and effects of CORT in response to stress are well established, the role of dehydroepiandrosterone (DHEA), another steroid that is released in conjunction with CORT, is not as clear. DHEA is a precursor in the production of the two main classes of sex hormones, androgens and estrogens (Labrie et al., 2005). Similar to glucocorticoids, circulating DHEA levels increase in response to ACTH production that results from HPA axis activation (Oberbeck et al., 1998). However, unlike the excitatory physiological roles of glucocorticoids, DHEA seems to have an antt-GC effect within the context of the stress response. In mice, DHEA protects neurons from degradation that results from excess GCs, as shown in the hippocampus of the animal's brain

(Karishma and Herbert, 2002). The mechanism of this is unclear, since DHEA does not have substantial binding affinity for GR or MR receptors and a DHEA receptor has not been identified, but it is possible that the synthesis of active sex steroids from DHEA may be a way in which the molecule balances the glucocorticoid-induced stress response.

DHEA is a precursor for testosterone, the male sex hormone, which is also influenced by circulating CORT levels. One of the roles of glucocorticoids during times of stress is to signal for reduction in reproductive system activity, allowing energy to be redirected to areas of immediate need such as skeletal and cardiac muscle (Leung and Munck, 1975). Thus, plasma testosterone levels are inversely related to plasma CORT levels, meaning that testosterone decreases when CORT levels rise (Tokarz et al., 2017). Therefore, during acute or chronic stress, when the HPA axis is producing high levels of glucocorticoids, testosterone levels are expected to decrease even with the increase in the hormone's precursor, DHEA.

Steroidogenesis

Steroid hormones, such as corticoids, progestins, androgens, and estrogens, are synthesized in a multi-step pathway that is highly regulated and involves multiple enzymes (Figure 2). These types of steroids are defined by the number of carbons in their rings; progestins have 21 carbons, androgens have 19, estrogens have 18, and corticoids have 21 (Henley et al., 2005). Progestins are essential for reproductive activity in all sexes, while androgens and estrogens cause the formation of male and female secondary sexual characteristics, respectively (Miller, 2013). Corticoids can be divided into two subclasses, glucocorticoids and mineralocorticoids. Glucocorticoids, cortisol and corticosterone, are mainly responsible for mobilizing glucose, while mineralocorticoids, such

as aldosterone, allow renal tubules to retain sodium to influence electrolyte and fluid balance (Henley et al., 2005).

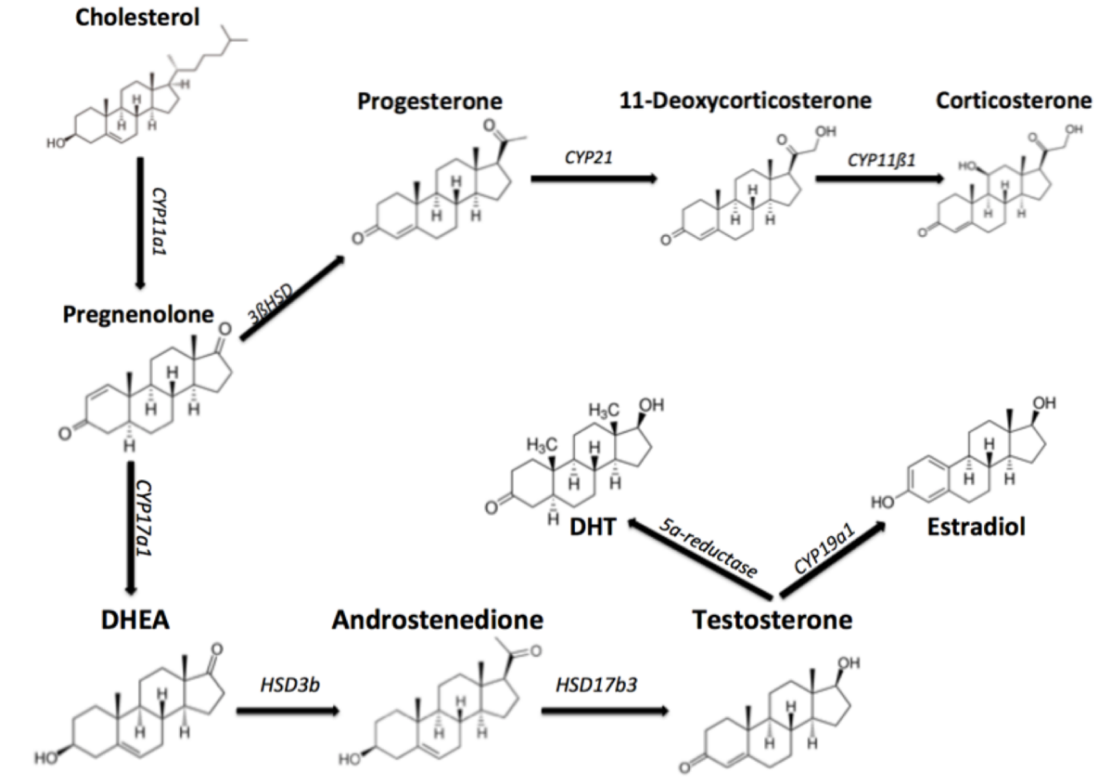

Figure 2. Synthesis of steroid hormones results from an enzymatic pathway that converts cholesterol into androgens and estrogens in a step-wise manner. The first step, in which CYP11a1 cleaves a cholesterol side chain (C27) to yield pregnenolone, is the rate-limiting step of all steroidogenesis reactions. Each step afterwards is done by a separate enzyme (gene name shown in italics) to yield various hormones or hormone pre-cursors (shown in bold). The structure of each substrate and product of the steroidogenic enzymes are shown.

De novo synthesis of each type of steroid begins with the conversion of cholesterol to pregnenolone in the inner membrane of the mitochondria by cleaving a side chain on cholesterol's 27th carbon to yield the 21-carbon molecule, pregnenolone (Miller, 1988). Pregnenolone is then converted to progesterone in both the mitochondria and smooth endoplasmic reticulum, after which both pregnenolone and progesterone act as precursors for other steroid hormones. The enzymes involved in each step of this process have been studied in the gonads and adrenal glands of many organisms, as these tissues are sites of high steroidogenesis activity (Sanderson, 2006).

The enzymes can be classified into two families: cytochrome P450 heme-containing proteins and hydroxysteroid dehydrogenases. The P450 enzymes, named with the prefix "CYP," are bound in either mitochondrial or endoplasmic reticular membranes and catalyze hydroxylation and cleavage of steroid substrates (Sanderson, 2006). Hydroxysteroid dehydrogenases, named with the prefix "HSD," are involved in redox reactions of steroid hormones and can take on multiple isoforms that are each a product of a separate gene (Payne and Hales, 2004).

StAR Protein

All steroid hormones are synthesized from a cholesterol precursor (Figure 2). The rate-limiting step of steroidogenesis is before the actual enzymatic process and involves the initial transport of cholesterol, from within the outer mitochondrial membrane, lipid droplets, or the plasma membrane, to the cytochrome P450-side chain cleavage enzymes (P450scc or CYP11A) located within the inner mitochondrial membrane (Stocco, 2000). The steroidogenic acute regulatory (StAR) protein mediates the delivery of cholesterol to P450scc. This protein is necessary because cholesterols are hydrophobic and cannot diffuse through the inner membrane of mitochondria from their origin outside the organelle, thus they require a transport protein. After transport, P450scc can convert the cholesterol to pregnenolone through the cleavage of its side chain (Stocco, 2000). In mice, pregnenolone levels have been shown to increase in response to stress, coinciding with the molecule's role in the biosynthesis of glucocorticoids and other steroid hormones (Holzbauer and Newport, 1967). StAR is a crucial enzyme for steroidogenesis, as shown in StAR knockout mice that developed congenital lipoid adrenal hyperplasia, a lethal disease caused by a blockage of steroid hormone production (Caron et al., 1997).

CYP17A1

After P450scc converts cholesterol to pregnenolone in the first enzymatic step of steroidogenesis, the resulting steroid is converted into precursors for androgens by the enzyme cytochrome P450 17a-hydroxylase/C17-20lyase (CYP17A1). This enzyme catalyzes two reactions, hydroxylation of pregnenolone or progesterone to 17-hydroxypregnenolone and the subsequent cleavage of the C17-20 bond to produce the steroid DHEA (Payne and Hales, 2004). As DHEA levels increase after acute stress, specifically in response to CRH release, it is likely that expression of CYP17A1 would also increase (Parker et al., 1999). Also, activation of the enzyme may increase during acute stress, rather than simply its expression. Cytochrome b5 is an allosteric effector of CYP17A1, increasing the maximum velocity of its enzymatic activity (Vmax), suggesting that CRH release could stimulate the availability of this cytochrome protein in order to increase steroid synthesis via CYP17A1 activity (Payne and Hales, 2004). The effects of DHEA are largely inhibitory to the HPA axis in order to prevent the negative effects of high glucocorticoid levels, which is the most likely explanation for the increase in DHEA levels during stress (Muller et al., 2006).

HSD17ß3

After conversion of pregnenolone into DHEA, androstenedione is synthesized from DHEA by the actions of the enzyme 3ßHSD in the mitochondrial membrane (Payne and Hales, 2004). Androstenedione, a weak androgen, is then converted to the more bioactive androgen, testosterone, by the enzyme 17b-hydroxysteroid dehydrogenase (HSD17ß3), essentially completing the main steroidogenesis pathway in male animals (Figure 2). Testosterone can then be further converted into a more potent androgen (DHT) or into estrogens (e.g., estradiol). HSD17ß3 is an essential enzyme because it catalyzes the last step in the synthesis of the male gonadal steroid hormone,

testosterone (Payne and Hales, 2004). This enzyme is different than the previously discussed P450 proteins because it is not a part of the production of adrenal steroids, but rather the conversion between two androgen forms. Also, HSD17ß3 functions to reduce oxidative agents, which differs from the hydroxylation and cleavage activities of P450 proteins (Payne and Hales, 2004). HSD17ß3 is almost always detected in the gonads of male organisms, as it is essential testosterone production, confirmed by in situ hybridization of mice testes (O'Shaughnessy et al., 2002). During stress, HSD17ß3 may decrease due to lowered production of testosterone during the inhibition of reproductive activity, a result of the stress response.

CYP19A1

Androgens can be converted into estrogens by cytochrome P450 aromatase (Coumailleau et al., 2014). Aromatase, which is encoded by the CYP19A1 gene, converts the C19 androgen, testosterone, into the C18 estrogen, estradiol, through the formation of an aromatic ring. This enzyme is mainly present in female preovulatory follicles, but has been detected in the male testes, especially during development (Durkee et al., 1992). Estrogens do not have a defined role in the stress response, so the expression of CYP19A1 in the gonads is likely to remain unchanged during stress. However, aromatase has been consistently found in the brain, showing that is has a neurological role in addition to its gonadal role (Coumailleau et al., 2014). In birds, aromatase activity levels in the diencephalon are positively correlated to aggressive behavior, suggesting that the conversion of testosterone to estrogen in the brain is key in activating aggression (Silverin et al., 2004).

Biosynthesis of Glucocorticoids

Outside the gonads (i.e., testes and ovaries) pregnenolone can take an alternate route in steroid biosynthesis that leads to adrenal glucocorticoid production (Figure 2). To synthesize

corticosterone, pregnenolone is first converted into progesterone by the enzyme HSD3ß (Payne and Hales, 2004). Progesterone is a progestin steroid hormone, making it crucial for reproduction, but is also an important metabolic intermediate in the formation of GCs. It is further converted into 11-Deoxycorticosterone by the enzyme CYP21 and this molecule is cleaved by the enzyme CYP11B1 to make CORT, the essential hormone in acute and chronic stress response (Payne and Hales, 2004).

CYP21 is expressed in the adrenal cortex and has not been found in kidney, liver, testis, or ovary tissues, confirming its role in adrenal production of CORT (Parker et al., 1985). Similarly, the expression of CY11B1 is also confined to the adrenal cortex (Curnow et al., 1991). However, the CORT produced in this adrenal biosynthetic pathway may influence the expression of other steroidogenic enzymes outside of the adrenal cortex. A study by Hales and Payne (1989) found that GCs negatively regulate the expression of StAR in mouse Leydig cells, the most potent cells in androgen synthesis. This suggests that the production of CORT, specifically in response to stress, may influence the synthesis of steroid hormones, such as testosterone, via regulation of the enzymes involved in the steroidogenic pathway.

Local Steroidogenesis

While the adrenal release of GCs has been extensively studied, recent research suggests that various organs may produce glucocorticoids and other steroid hormones via localized HPA axes in specific tissues (Taves et al., 2011). This phenomenon is known as local steroidogenesis and is gaining increasing prominence as an overlooked component of the endocrine system. Steroids that are produced *de novo* in specific organs can alter local concentrations and result in rapid binding to receptors, enhancing the speed of the systematic stress response by bypassing the need for hormones to travel through the blood stream.

In the brain, androgens and estrogens can be made *de novo* from cholesterol precursors, similar to the steroidogenic pathway in the adrenal gland, or from DHEA precursors that are circulating in the blood (Sawada et al., 1998). These hormones protect neurons against degradation, making them vital in the brain and supporting the probability that the steroids may be synthesized locally. Cholesterol for neural steroid synthesis may come from circulating lipoproteins or myelin and plasma membranes, with the latter being more likely since cholesterols in lipoproteins cannot cross the blood-brain barrier (Korade and Kenworthy, 2008).

Steroidogenic enzymes have been found in the brain, which supports the hypothesis of local steroid synthesis. StAR is expressed in neurons and glia in certain regions of the brain, indicating possibility of *de novo* synthesis since this enzyme is required for the transport of cholesterol to begin the steroid production process (King et al., 2004). The brain is an ideal organ to begin the study of local steroidogenesis because it is already involved in signaling for adrenal steroid production, but other tissues have not been as extensively studied. The steroidogenic enzymes CYP11 and HSDß3 were found in human cardiac tissue in a study by Kayes-Wandover and White (2000) and CYP19 has been detected in human adipose tissue by Simpson et al. (2002), but no studies have provided comprehensive evidence for the expression of multiple steroidogenic enzymes in various tissues of one organism.

The objective of the current study is to determine whether steroidogenic enzymes are expressed across a suite of organ tissues of brown anole lizards (Anolis sagrei), which could signify local steroid synthesis, and to determine whether the stress associated with fasting influences the gene expression of steroidogenic enzymes.

The Brown Anole as a Model Organism

The current study used brown anoles (*Anolis sagrei*) as the model organism for investigating local steroidogenesis and for testing the effects of fasting on the expression of steroidogenic enzymes in various tissues. Brown anoles are an invasive lizard species in the southeastern United States, originally from Cuba and the southern islands of the Bahamas, and they are particularly abundant in Florida (Manthey et al., 2016). This species is also closely- related to another model species in endocrinology, behavior, and physiology, the US native green anole (*Anolis carolinensis*) (Figure 3). The abundant research on these species provides a valid framework for addressing our study in an ecological context.

Anoles are highly territorial and rely on dominant relationships to determine social status in a population, which is linked to the adrenal stress-response. Male brown anoles that have a lower status exhibit subordinate behavior and have significantly increased CORT levels after an aggressive encounter with a dominant lizard (Greenberg et al., 1984). This observation suggests that CORT inhibits male aggressive behavior in the brown anole, which was confirmed by the decrease in the aggressive response (erection of a crest or biting behavior) of animals that were given chronic CORT treatment (Tokarz, 1987). This could occur because of direct impact of CORT on aggressive motivation in the brain via ACTH release, but is most likely the result of the negative effect of increased CORT on plasma testosterone levels. ACTH has been shown to decrease aggressive behavior in mice, but similar results have not been established in reptiles (Leshner, 1980). Decrease in testosterone levels in response to CORT treatment, however, has been established in brown anoles and is supported by decreased testis weight and spermatogenesis following CORT treatment (Greenberg et al., 1984). Thus, the brown anole is an excellent model

for studying local steroidogenesis because the animal consistently shows the adrenal response that results in CORT production and similar mechanisms can be studied in other organs.

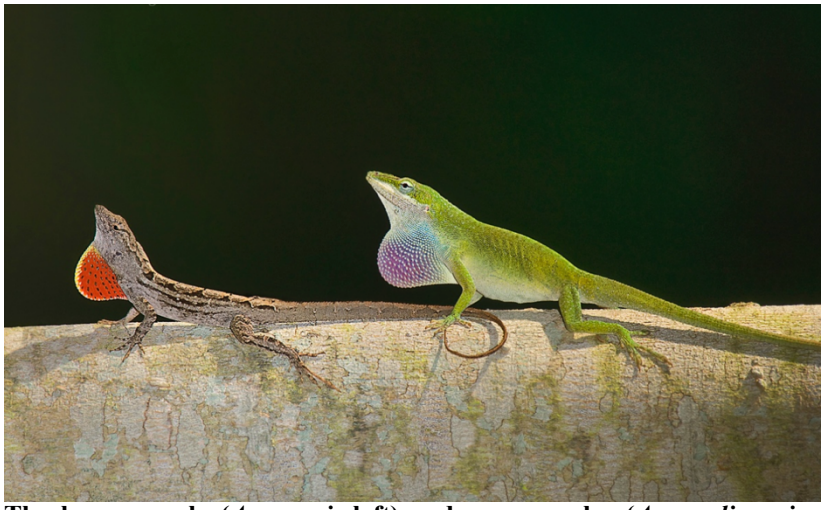

Figure 3. The brown anole (*A. sagrei;* left) and green anoles (*A. carolinensis;* right) are physiologically very similar, as seen by their appearance and display of aggressive behavior. Both species of Anolis are shown displaying their dewlaps as a sign of aggression, as a result of either a territorial or physical threat (Losos, 2014).

Anoles could be ideal models for studies of steroidogenic gene expression patterns because the entire genome of the green anole has been sequenced and assembled from its DNA (Alföldi et al., 2011). This allows for sequence-specific identification of gene expression in a tissue sample via mRNA (messenger RNA) extraction and RT-PCR amplification. Although the brown anole genome has not been sequenced, gene identification can be derived from the green anole genome, as these two species are of the same genus. However, the green and brown anoles have a slightly diverse evolutionary relationship, which may cause imperfect primer design for RT-PCR (Figure 4). The green anole genome is the closest sequence available for studying brown anole mRNA, so sequences of green anole genes will be used to design RNA primers to amplify brown anole genes.

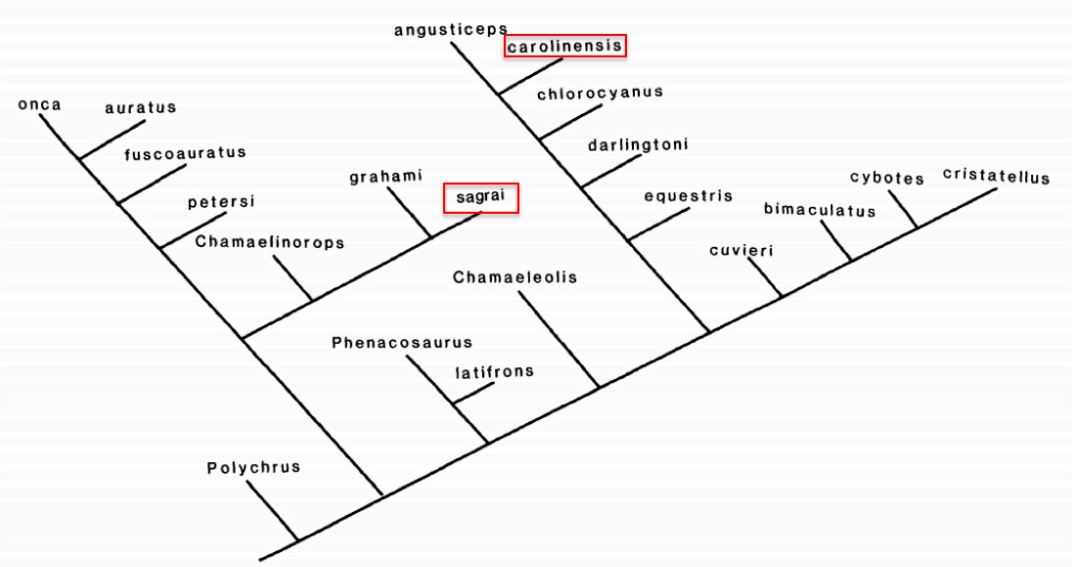

Figure 4. The phylogenetic tree for Anolis lizards shows the diversity of brown anoles (*A. sagrei*) and green anoles (*A. carolinensis*). Terminal taxa all have the genus *Anolis*, with various species shown as branches (Guyer and Savage, 1986). This tree was obtained via molecular and morphological date of each species.

Experimental Aim: Determination of Local Steroidogenesis

To determine the effects of fasting on local steroid synthesis in brown anoles, RNA was extracted from previously harvested tissues of anoles that were either fasted or fed regularly. Gene amplification of steroidogenic enzyme-coding genes, using RT-PCR will be performed using the extracted RNA. Relative quantification of mRNA expression and confirmation of primer specificity will be determined via DNA gel electrophoresis and UV transillumination for imaging, followed by qRT-PCR (SYBR Green) for precise quantification. The enzymes being measured include CYP19A1, StAR, CYP171A, HSD17ß3, and ß -actin as a control. The tissues from which mRNA was extracted are from brown anole brain, heart, lungs, liver, stomach, intestines, adrenals, pancreas, testes, kidneys, fat, muscles, and hemipenes. It is hypothesized that each tissue will exhibit local steroid synthesis as a result of localized HPA axis effects, resulting in detectable steroidogenic enzymatic mRNA expression in fasted and control organisms. The adrenals, gonads, and brain will serve as positive controls because these organs are known to have steroidogenic

activity, thus genes for steroidogenic enzymes will undoubtedly be expressed, and the amounts of expression will be used as the standard "basal" steroidogenic activity level in a tissue. Expression of StAR and CYP17A1 mRNA is expected to be higher in fasted lizards, due to stress increasing the need for CORT and DHEA production, and expression of HSD17b3 and CYP19A1 should decrease in fasted lizards, due to the negative effects of CORT on the reproductive system and testosterone production.

Methods

Anole Treatments and Tissue Collection

Prior to the current study, brown anoles were collected from Winter Park, Florida, and acclimated to captivity for a week. Anoles were randomly assigned to either be fasted for one week or fed two large crickets every two days (control). Fasted and control anoles were then sacrificed and their tissues (adrenal gland, blood and plasma, brain, heart, lungs, liver, stomach, intestine, pancreas, kidney, testes, hemipenes, and muscle) were collected and preserved in RNAlater solution (Thermo Fisher Scientific, AM7020, Waltham, MA), which permeates tissues to immediately stabilize RNA in cells and protect against degradation. Samples were stored at -80ºC until analyzed (approximately two years).

Primer Design Analysis

Forward and reverse primer sequences required to amplify five genes (CYP19A1, CYP17A1, StAR, HSD17ß3, and ß-actin) in brown anole mRNA were obtained from Peek (2017) and are shown in Table 1. Primers were first analyzed for length, which ideally should be 18-22 nucleotides to allow for specificity and efficient binding to template, and for GC content, which should be between 30-80%, to allow for a high enough melting temperature to avoid complete degradation, but a low enough melting temperature to avoid secondary annealing and nonspecific

amplification. Then, primers pairs were analyzed for dimerization and self-dimerization abilities using Multiple Primer Analyzer software (Thermo Fisher Scientific). All primers were also analyzed for homology to possible non-target gene sequences using National Center for Biological Information (NCBI) BLASTn and were aligned with target genes using Clustal Omega software (EMBL-EBI). NCBI BLASTn was used to align primers to the mapped green anole genome to determine if the sequences spanned predicted splice sites in order to confirm specificity for mRNA and not gDNA.

Table 1. Forward and reverse primer sequences for amplification of each target gene in brown anole tissue samples (Peek 2017). Melting temperatures of each primer were found using Taq Polymerase parameters (NEB Tm Calculator) and expected amplicon size of each gene are included.

Gene	Amplicon Size (bp)	Primer Sequences	Melting Temperature
StAR	112	F: CACTCGCTGGAGATCCCTACC R: TCCACCTGCGTCTGGG	F: 58.3ºC R: 51.1ºC
CYP17A1	86	F: GGGAACCGAATCTACAGCCC R: ATCTTGGCTAGCGCTTTCC	F: 55.9ºC R: 51.1ºC
CYP19A1	90	F: CCAGGTCTTGTGCGGATGAT R: GTAGCCACACTTGGTGGTCA	F: 53.8ºC R: 53.8ºC
HSD17ß3	71	F: GTGGGGGTAAGGACAGTCAC R: CAGAAGGGCATTTTTGGCCC	F: 55.9ºC R: 53.8ºC
ß-Actin	131	F: GACGAGGCGCAGAGTAAAAG R: TCAGGGGCAACTCTCAACTC	F: 53.8ºC R: 53.8ºC

RNA Extraction

Brown anole tissue samples in RNAlater solution were thoroughly dried with paper towels and homogenized in Trizol (1mL/50mg tissue) at 5500 rpm for 20 seconds with 2.3 mm zirconia/silica beads in a Precellys 24 homogenizer (Bertin, EQ03119-200-RD000.0, Paris, France). Chloroform (0.2X) was added, the solution was incubated for three minutes at room temperature, and then centrifuged at 12,000 x g for 15 minutes at 4ºC. After another centrifugation

at 12,000 x g for 15 minutes at 4ºC, the aqueous phase was combined with isopropyl alcohol (0.5 mL/1 ml Trizol), incubated for 10 minutes at room temperature, and centrifuged at 12,000 x g for 10 minutes at 4ºC. The pellet was washed with 75% ethanol (1X), centrifuged at 7,5000 x g for 5 minutes, and resuspended in RNase free water. Samples were stored at -80ºC until further analysis.

RNA Integrity Testing

Extracted RNA was tested via gel electrophoresis to confirm absence of contamination and/or degraded RNA, as well as accuracy of spectrophotometric quantification. After quantification via UV/Vis spectroscopy (Thermo Scientific Nanodrop 1000), 500 ng of each sample was loaded on a 1% agarose gel with 1% bleach in 1X TAE. Electrophoresis was run at 100V for 15 minutes, to avoid overheating and denaturing of RNA, and then 150V until complete.

Primer Specificity Testing

To confirm primer specificity, RT-PCR was performed for each gene and reactions included 1X OneTaq One-Step Reaction Mix (New England Biolabs, E5315S, Ipswich, MA), 1X OneTaq One-Step Enzyme Mix (NEB), 0.4µM each gene-specific forward and reverse primer (NCBI), and 500 ng template RNA. RT-PCR conditions included 30 minutes at 48ºC (RT reaction), one minute at 94ºC (initial melting), 40 cycles of melting (one minute, 94ºC), annealing (30 seconds, 55ºC), and extension (30 seconds, 68ºC), and finally five minutes at 68ºC (final extension) with an indefinite hold at 4ºC. Additional RT-PCR reactions were done to amplify HSD17 ß 3, using the same parameters, except annealing temperature was raised to 60ºC to determine optimal conditions for the amplification of the gene. Amplified cDNA, made using the original RT-PCR conditions, was analyzed for concentration and purity via nanodrop and DNA agarose gel electrophoresis using a 2% agarose gel in 1X TAE (100 V for 45 minutes). Samples were extracted from the agarose gel and sent for sequencing to confirm reverse transcription and

amplification of the correct genes. Only genes that were successfully amplified with this primer set (i.e. showed a clean single band after electrophoresis and produced amplicons homologous to the target gene sequence) were used for further study.

cDNA Synthesis for qPCR Preparation

RNA extracted from anole brain tissue was reverse-transcribed into cDNA for use in qPCR amplification using a Superscript IV Reverse Transcriptase kit (Thermo Fisher Scientific, 18090010, Waltham, MA). Reactions included Oligo $d(T)_{20}$ primers (2.5 µM), dNTP mix (0.5 µM), 5X SSIV Buffer (1X), DTT (5mM), ribonuclease inhibitor (0.05X), and SuperScript IV Reverse Transcriptase (200U) up to a final volume of 50 µL. Primers were annealed to RNA prior to reverse transcription reaction, as per manufacturer's instructions. Purity and concentration of cDNA was tested via nanodrop.

qPCR Primer Concentration and cDNA Dilution Optimization

Brown anole brain cDNA was used to optimize primer concentrations and cDNA dilution for qPCR amplification of ß-actin, CYP17a1, and StAR genes using Power SYBR Green PCR Master Mix (Thermo Fisher Scientific). Primers for ß -actin were tested first, with forward: reverse primer ratios of 1:1, 1:7, 7:1, 7:7, 8:1, and 9:1, in which "1" represents 2.5µM of primer, "7" represents 17.5mM, "8" represents 20µM of primer, and "9" represents 22.5µM. Both 1:20 and 1:40 dilutions of cDNA were also tested in order to determine if more dilute cDNA would contain enough molecules to be amplified effectively. Reactions for each primer ratio were run in triplicate, as well as no-template controls (NTC), and each set of reactions was run for each cDNA ratio. Standard qPCR parameters of 95ºC for 10 minutes, 95ºC for 15 seconds, and 65ºC for one minute (40 cycles) were used. Each reaction included 2.5X Master Mix and either 121 ng cDNA (1:20 ratio), 60 ng cDNA (1:40 ratio), or sterile RNase free water (NTC).

Primers for CYP17a1 and StAR genes were then tested, using the optimized 1:40 dilution of cDNA and 1:1, 1:7, 7:1, and 7:7 forward: reverse primer ratios. Reactions were again run in triplicate with NTCs. The same qPCR parameters were used, but with only 35 cycles and an annealing temperature of 62ºC.

Samples of amplified cDNA from qPCR reactions were analyzed via electrophoresis on a 2% w/v agarose gel in 1X TAE (100V for 45 min) to confirm amplification of the correct product and assess presence of primer dimers. Step-One Plus Expression Suite Software (Thermo Fisher Scientific, 4376600, Waltham, MA) was used to determine Ct values and analyze melt curves for all qPCR samples.

Results and Discussion

Primer Analysis

NCBI BLASTn is a tool that uses an algorithm to match an input sequence, in this case forward and reverse primers, to any and all sequences in a gene database (Altschul et al, 1990). NCBI Blast searches of each primer confirmed 100% homology to their respective predicted gene sequences, indicating that they would perfectly bind to the green anole RNA sequence of each gene in this study [Figure 5]. Furthermore, Blast revealed that primers have no significant homology to locations in the green anole genome aside from the target genes, indicating a low risk for non-specific amplification. Since the brown anole genome has not been mapped, it is impossible to design primers specific for that species. Thus, it is possible, if not likely, that the primers do not perfectly base pair to the intended target in the brown anole genome.

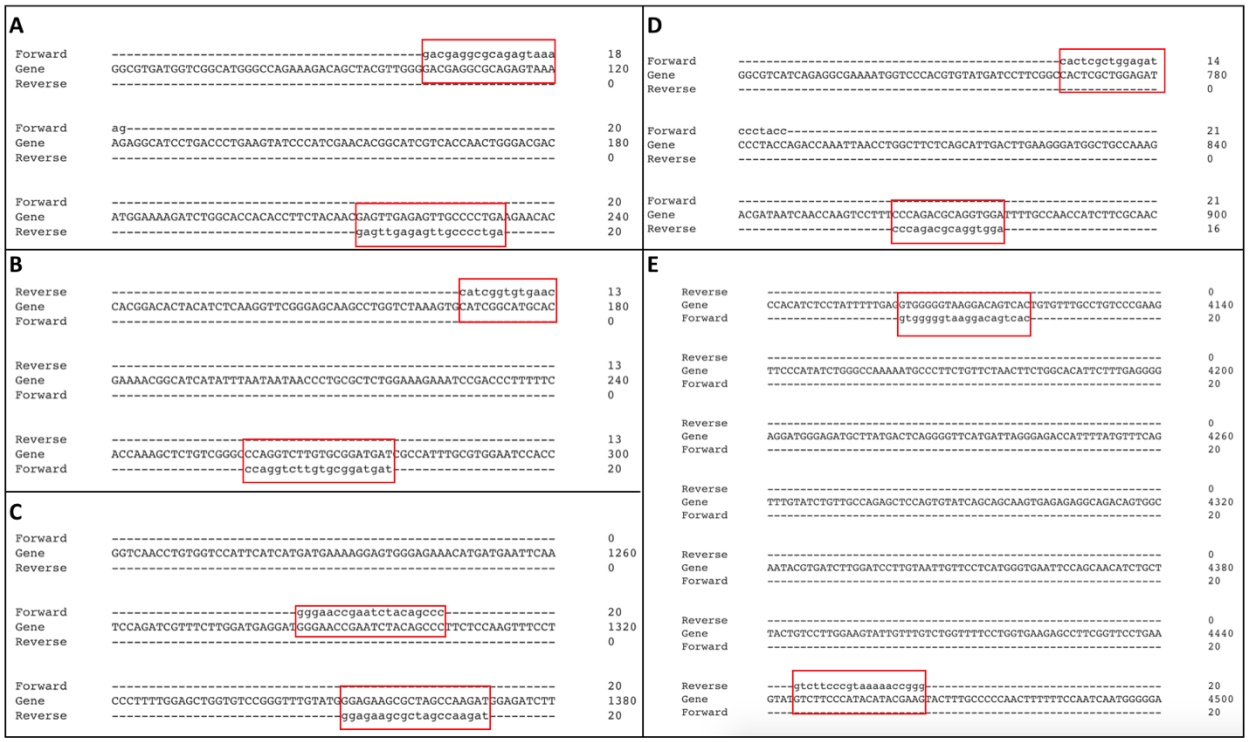

Figure 5. Nucleotide sequence alignment of PCR primers with each predicted gene sequence of green anole mRNA shows that forward and reverse primers are specific for the five genes of interest. Red boxes indicate forward and reverse primer sequences that are 100% homologous to predicted gene sequences. A) ß-actin gene. B) CYP19a1 gene. C) CYP17a1 gene. D) StAR gene. E) HSD17ß3 gene. All alignments were created via Clustal Omega (EMBL-EBI).

Further analysis also confirmed that all primers crossed exon-exon boundaries on mRNA. This is important for RT-qPCR, because a primer that is completely contained within an exon has the ability to bind to genomic DNA (gDNA), as gDNA contains introns that are removed by splicing during the formation of mRNA (Ye et al., 2012). Unwanted amplification of gDNA would interfere with quantification of mRNA in qPCR, producing unreliable data. Primers should be designed to span an exon-exon junction so that they would not be able to completely bind gDNA, as the binding sequence would be disrupted by an intron. Each primer sequence was aligned with the mapped gDNA of the green anole, and it was confirmed that none of the sequences aligned, meaning that the sequences are specific for mRNA.

Finally, analysis of primer-dimer expectancy showed none of the primer sets had self-dimer or primer-dimer capabilities except the StAR primer set, which had one self-primer possibility in the forward primer. Primer dimers occur when forward and reverse primers designed for the same gene have the ability to complementarily bind to each other and self-dimers occurs when one primer has at least two portions that can complementarily bind. In both scenarios, the binding of primers makes them unavailable to bind to the template RNA and thus affects amplification and quantification. Also, amplification of primer dimer and self-dimers could result in false quantification, as they would be included in the mRNA amplification yield.

RNA Integrity

RNA extracted from brown anole tissues was examined for quality and quantity via bleach gel electrophoresis and UV absorbance (260 and 280 nm). Bleach gel electrophoresis is done to assess RNA samples for degradation and contamination. The addition of bleach to a 1% agarose gel serves as a denaturing agent that disrupts secondary structure of RNA, allowing for accurate analysis of fragment sizes (Aranda et al., 2012). The bleach also destroys RNases that may have contaminated the gel to prevent unwarranted degradation of samples, which could interfere with analysis (Hawkins and Davies, 1998). The desired result of electrophoresis is the presence of two clean bands in each sample that represent rRNA (ribosomal RNA) of the 28S and 18S ribosomal subunits, with the former being larger and showing twice the intensity of the latter (Cizdziel and Chomczynski, 1996). Intact and un-contaminated RNA presents as crisp bands with no smearing. Smearing of samples below the rRNA bands indicates degraded RNA, as short oligonucleotide fragments would run at low molecular weights, while smearing above the rRNA bands usually indicates contamination by proteins, phenol, or gDNA (Carvalhais et al., 2013).

The first set of RNA extractions, done prior to a change in protocol, showed many samples with smears above rRNA bands on the bleach gel, indicating contamination [Figure 6]. The most likely cause of contamination was Trizol reagent, as indicated by low 260/230nm absorbance ratios [Table 2].

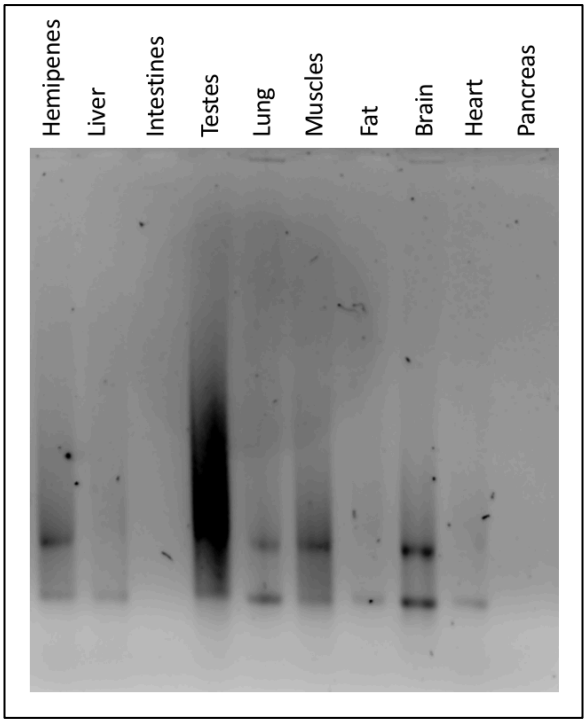

Figure 6. RNA extracted from various brown anole tissues had high levels of contamination, but nearly no degradation, as shown by bleach gel electrophoresis. 500 ng of each RNA sample were run on a 1% bleach agarose gel in 1X TAE. Two distinct bands for each sample that represent 23S (top) and 16S (bottom) rRNA were expected for each sample. Samples shown correspond to samples labeled "11" in Table 2.

Nucleic acids present in RNA have an absorbance peak at a wavelength of 260 nm, while the phenol present in Trizol has its peak at 230 nm (Thermo Fisher Scientific, 2009). The 260/230 nm ratio of RNA samples should ideally be between 2.0-2.22, which indicates minimal expected phenol contamination (Gayral et al., 2011). Protein did not seem to be a contaminant, as concluded by the mostly acceptable 260/280 nm ratios of the samples [Table 2]. This ratio, which is ideally around 1.8, represents protein contamination because proteins have a peak absorbance at 280nm (Desjardins and Conklin, 2010).

Table 2. Concentration and purity of RNA extracted from brown anole tissues. Absorbance at 260/280 nm corresponds to protein contamination level and absorbance at 260/230 nm to Trizol contamination level. Samples in bold were extracted with an optimized protocol.

Brown Anole Tissue Sample	Concentration (ng/µL)	Absorbance (260/280 nm)	Absorbance (260/230 nm)
Lung 11	245.8	1.79	*N/A*
Testes 11	4489.8	1.16	0.69
Intestine 11	3327.2	1.90	*N/A*
Liver 11	978.3	1.59	0.62
Hemipenes 11	1255.7	1.54	0.67
Stomach 11	182.2	1.63	*N/A*
Muscle 11	489.2	1.63	0.39
Pancreas 11	4175.4	1.74	*N/A*
Fat 11	257.3	1.58	*N/A*
Brain 11	2052.9	1.90	*N/A*
Heart 11	232.5	1.66	*N/A*
Brain 6	**166.1**	**1.90**	**1.57**
Brain 14	**128.4**	**1.80**	**2.34**
Brain 4	**91.7**	**1.79**	**1.68**
Brain 5	**16.0**	**1.76**	**0.82**

Most samples from the first set of RNA extractions were contaminated, with the RNA from the testes having the most contamination, as indicated by streaking along the entire length of RNA migration on the gel [Figure 6]. There was no degradation of RNA in the samples, which would have been indicated by smearing below the two bands that corresponded to the 23S and 16S rRNA. Since all samples had degradation above these bands and nanodrop readings that indicated no protein contamination, the primary contaminant was assumed to be phenol. The high phenol contamination is most likely a result of the unnecessarily high concentration of Trizol used in the extraction procedure. The recommended amount of Trizol when extracting RNA is 1 mL per 50-100 g of tissue, but the initial procedure used 1mL of Trizol for each sample, regardless of tissue amount. Since the tissues being used were often much less than 50 g, there was a large amount of extra Trizol in the samples, leading to contamination of the final product. Another possible contaminant that could have caused smearing on the bleach gel was genomic DNA (gDNA), as

this would have run above the rRNA bands at nonspecific molecular weights. In addition, some tissue samples did not have detectable levels of RNA at all, such as the pancreas and heart [Figure 6]. Organs with large amounts of contractile proteins, connective tissue, and/or collagen, like the heart, have been shown to have low RNA yields due to the abundance of these tough tissues and proteins (Gayral et al., 2011). In addition, the pancreas typically has a low RNA yield due to an abundance of nucleases in the tissue (Cizdziel and Chomczynski, 1996).

The second set of RNA extractions, which included slight modifications to the original protocol, revealed much cleaner RNA samples. First, the amount of Trizol used was adjusted for the weight of each tissue sample to reduce addition of unnecessary phenol that may have been contaminating the final product. Also, an extra centrifugation step was added after extracting most of the RNA-containing supernatant from the separated phenol-chloroform samples. This was done to ensure that all protein contaminants and phenol were separated completely so that only pure RNA in the aqueous layer of each sample was collected. This second set of samples were from brain tissues of four different brown anoles, as the previous RNA extraction from brain tissue showed the most distinct rRNA bands out of all tissue samples. Three samples produced clean and abundant RNA, as shown by distinct bands that corresponded to 28S and 18S rRNA and relatively no smearing [Figure 7]. One sample, although not contaminated, had a very low yield and thus was not viable for further experimentation [Figure 7]. The UV absorbance values of each sample confirmed absence of Trizol contamination, shown by 260/230 ratios, as well as high yield and

lack of protein contamination, as shown by 260/280 ratios, aside from the low yield and larger presence of protein in one sample [Table 2].

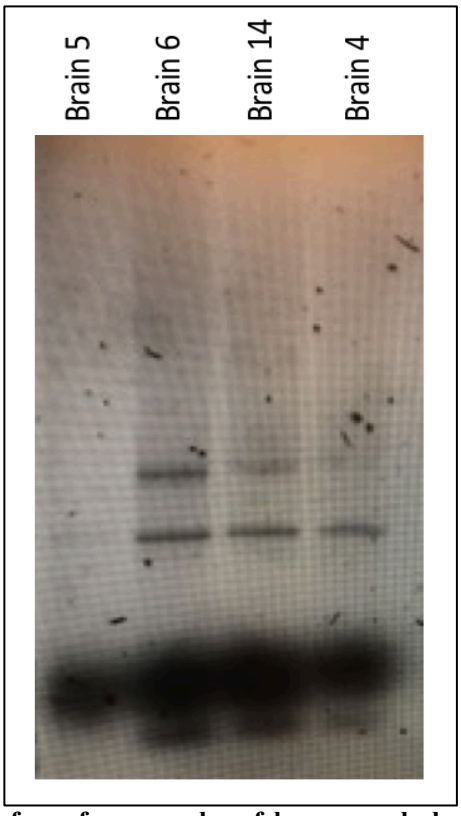

Figure 7. RNA extracted from four samples of brown anole brain tissue had little to no contamination and nearly no degradation, as shown by bleach gel electrophoresis. Equal volumes of each RNA sample were run on a 1% bleach agarose gel in 1X TAE. RNA extracted from brain tissue of organism 5 had a low yield as compared to other samples. Dye front can be seen at the bottom of the gel, as well as bands of tRNA. Two distinct bands for each sample that represent 23S (2906 bp) and 16S (1542 bp) rRNA were expected for each sample.

Primer Specificity

Before attempting quantification of genes, the specificity of RNA primers were tested by amplifying each target gene via one-step RT-PCR. The RNA template used was extracted from the testes and amplified products were run on a 2% agarose gel. The primers successfully amplified CYP17a1, StAR, and ß-actin genes, as shown by bright bands on the gel that corresponded to the expected amplicon size of each gene [Figure 8]. However, CYP19a1 and HSD17ß3 did not bear similar successful results. CYP19a1 did not appear to amplify at all in this sample, while HSD17ß3

primers produced amplicons of various sizes [Figure 8]. The lack of amplification of CYP19a1 may be from faulty primers, but because the primers had 100% homology to the gene, the more likely cause was low abundance of the gene in the RNA template. This is expected because CYP19a1 encodes for the enzyme aromatase, which converts androgens into estrogens (Simpson et al., 2002).

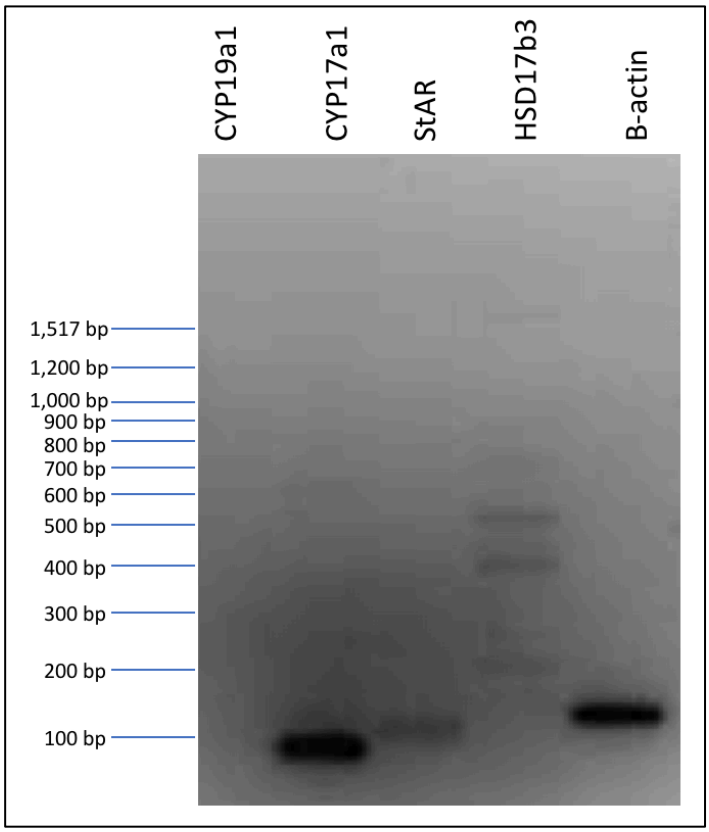

Figure 8. One-step RT-PCR using brown anole testes RNA successfully amplified cDNA of CYP17a1, StAR, and ß-actin genes, while amplification of CYP19a1 and HSD17ß3 genes was unsuccessful. RT-PCR reactions with CYP17a1, StAR, and ß-actin specific primers produced single amplicons, while HSD17b3 primers amplified brown anole RNA in fragments and CYP1a1 was not amplified. Expected amplicon sizes can be found in Table 1.

Since the template RNA was extracted from the testes of a male brown anole, which has little to no estrogen, it is reasonable that aromatase is not needed and therefore its coding mRNA is scarce or completely absent (Henley et al., 2005).

Multiple amplicons resulting from the HSD17ß3 primer set may have been caused by unfavorable RT-PCR conditions, alternative isoforms causing variation in mRNA sequences, or non-specific primers. In an attempt to improve RT-PCR conditions, the annealing temperature was increased from 55ºC to 60ºC to promote specific binding of primers to template RNA. Annealing temperature is usually set to five degrees less than the melting temperature of the primers, but can be increased by a few degrees to increase stringency of primer binding (Malhotra et al., 1998). This was unsuccessful, however, as seen by a continued production of non-specific bands despite changes in annealing temperature [Figure 9].

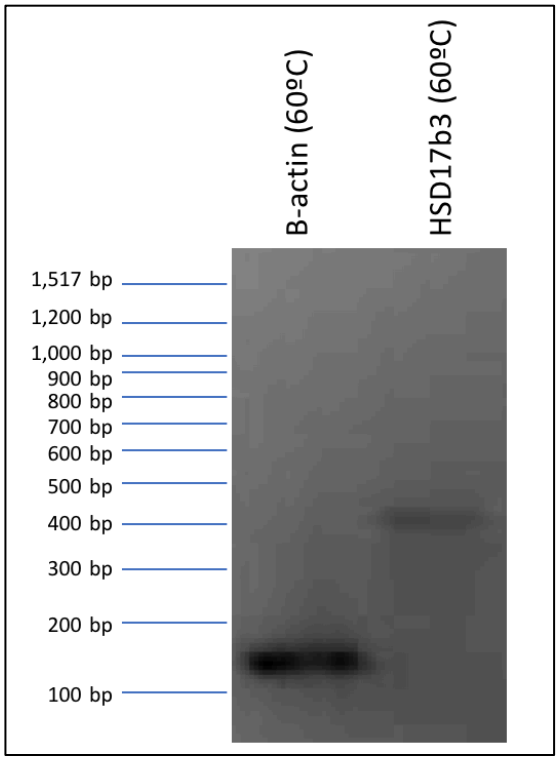

Figure 9. Change in annealing temperature during one-step RT-PCR was not successful in producing amplified cDNA (using RNA extracted from brown anole testes) of the HSD17b3 genes. RT-PCR reactions using 60ºC annealing as opposed to 55ºC did not produce a single amplicon of the expected size for HSD17b3 (71 bp). B-actin was amplified as a control and successfully produced the expected product (131 bp).

Another possibility for multiple products was that there are multiple isoforms of the HSD17ß3 enzyme family, which could have sequence homology at the primer-binding sites. This

seems reasonable because the HSD17ß isoforms, including HSD17ß3, are all expressed in the gonads and all function as similar enzymes, indicating that they may have similar polypeptide sequences and thus DNA sequences (Penning, 1997). However, the isoforms are encoded by distinct genes with unique polypeptide sequences that are specific to their location in the cell (Mindnich et al., 2004). There are a few conserved motifs, but otherwise HSD17ß3 enzymes have sequence homologies as low as 20% (Mindnich et al., 2004).

The least likely cause for the multiple amplicons, non-specific primers, must also be taken into consideration. Using NCBIn Blast, the HSD17ß3 primers showed 100% homology to the predicted green anole sequence for the target gene and no homology to any other part of the genome, which in theory means that there are no possibilities of non-specific binding on the template RNA. However, there is no way to confirm the primers' homology to the brown anole gene sequence, which is where the template RNA was extracted from, as the organism's genome has not been sequenced and mapped. Therefore, although the green and brown anoles are closely related, there could be a crucial few nucleotide difference in this gene that resulted in an inability of the primers to complementarily base pair to the template RNA at the target sites.

To confirm specificity of primers beyond DNA fragment sizes, reverse-transcribed amplicons of CYP17a1, StAR, and ß-actin genes were sequenced. NCBI Blast results of portions of the sequences confirmed that each sample contained DNA that is homologous to each target gene [Figure 10]. Only these three genes were chosen for sequencing because CYP19a1 primers did not produce enough of an amplicon to remove from the agarose gel post-electrophoresis and HSD17ß3 primers did not produce a single amplicon of the expected size.

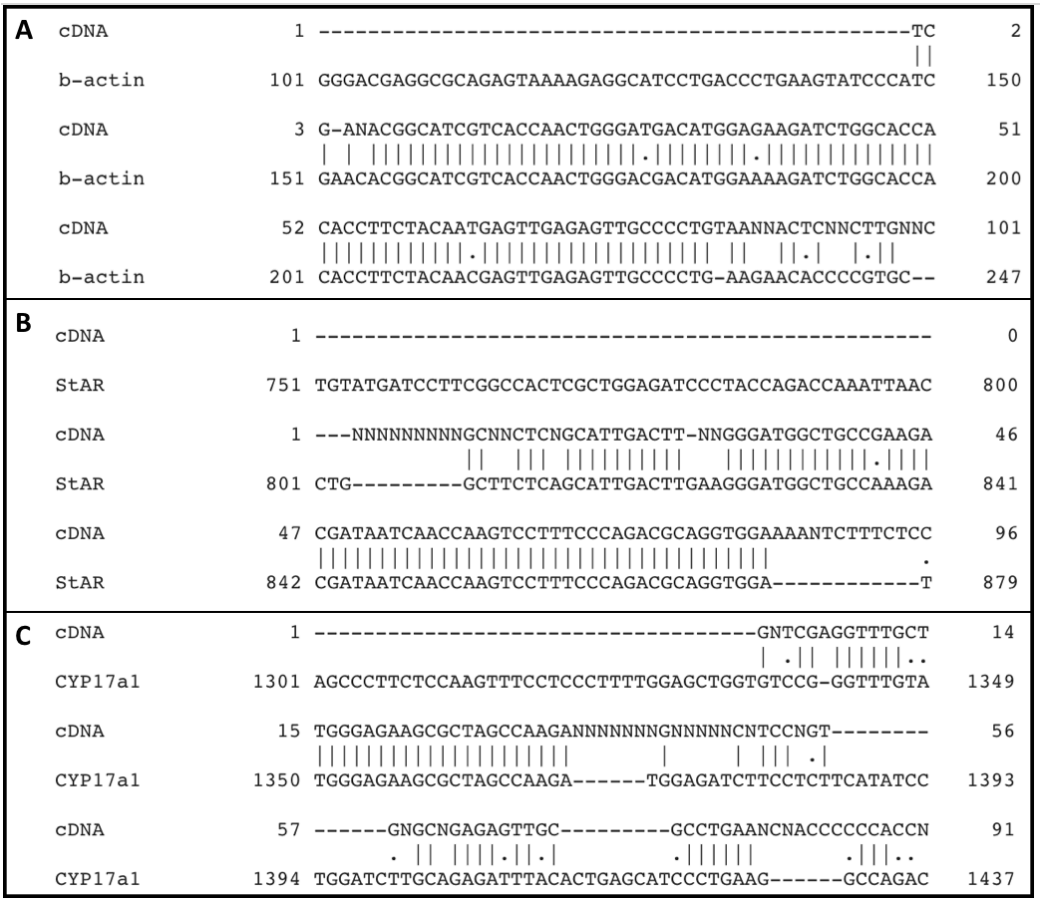

Figure 10. Pairwise sequence alignment of results obtained from sequencing brown anole cDNA and predicted sequences of three genes (A: b-actin, B: StAR, and C: CYP17a1) in the green anole genome show that primers used to make cDNA successfully amplified the correct genes. Each predicted gene sequence has substantial homology to the amplified cDNA made from RNA extracted from brown anole tissue. Sequence alignment was done via EMBOSS Needle (EMBL-EBI).

qPCR Primer Optimizations

To prepare RNA for qPCR, three samples extracted from brown anole brain tissue were reverse-transcribed into cDNA using Oligo$(dT)_{20}$ primers. These primers consist of a 20 nucleotide string of deoxythymidines and were chosen because they are specific for mRNA, as they complementarily bind to the poly-A tails that are exclusively found on the 3' end of mature eukaryotic mRNA (Kang et al., 2012). The concentration and purity of each cDNA sample was measured via nanodrop and all samples had high yields of pure cDNA [Table 3].

Table 3. Concentration and purity of cDNA made from RNA extracted from brown anole tissues. Absorbance at 260/280 nm corresponds to protein contamination level and absorbance at 260/230 nm to Trizol contamination level.

Brown Anole Tissue Sample	Concentration (ng/µL)	Absorbance (260/280 nm)	Absorbance (260/230 nm)
Brain 6	2424.9	1.73	1.86
Brain 14	2098.1	1.75	1.80
Brain 4	2393.5	1.75	1.79

Forward and reverse primer concentrations for each gene were optimized for qPCR using a sample of cDNA from the same brain tissue to find the ratio of forward: reverse primers that produced the lowest threshold cycle (Ct) values, with low standard deviations between replicates, and low levels or complete absence of primer dimers, all while producing the expected specific amplicon. This optimization procedure is done to ensure efficient and accurate qPCR assays, as standard primer concentrations are not always suitable for every target gene and have been shown to have only a 12% success rate when compared to optimized concentrations (Mikeska et al., 2009). The Ct value is the number of PCR cycles that are needed to exceed a threshold value that represents the point at which fluorescence signal surpasses background noise (Caraguel et al., 2011). A low Ct value is desired not only because it conventionally represents a high amount of target gene in the sample, but because a high Ct may indicate nonspecific amplification of background nucleotides and/or degradation of the fluorescent probe. Generally, the Ct values of target gene qPCR samples should be much lower than those of non-template controls, which should theoretically have an undetermined Ct (as there is no template to be amplified), but may have very high Ct values that correspond to the aforementioned free nucleotide amplification or probe degradation (Caraguel et al., 2011). A low standard deviation between replicates is desired to ensure reproducibility using the determined primer concentrations and absence of primer dimers

is needed to ensure accurate quantification of target gene amplification, uninfluenced by unwanted quantification of primer dimers.

Primer dimers can be identified via analysis of the melt curve for each qPCR sample. A melt curve shows the abundance of amplicons from qPCR that melt at a specific temperature, represented as a peak on the graph. The range of melting temperatures of most possible PCR products spans about 50ºC, allowing almost any amplicon to produce a unique peak on a melt curve (Ririe et al., 1997). An ideal qPCR reaction that is meant to amplify one target gene will have a single peak on the melt curve, representing that target gene. If there are primer dimers, there will usually be a second peak at a lower melting temperature than the target gene, due to the smaller size of the primer dimer resulting in less energy (temperature) required to melt it (Ririe et al., 1997).

The first qPCR run using ß-actin primers was overall unsuccessful. The primer concentrations tested in this run were 1:1, 1:7, 7:1, and 7:7 forward: reverse primer ratios. First, there was constant amplification of the NTCs, as shown by a clear peak on the melt curves of each replicate, which indicates contamination either by template cDNA or exogenous gDNA [Figure 11A]. The NTCs did produce Ct values that were higher on average than those of the cDNA-containing reactions, but they were not high enough to dismiss as background amplification [Figure 12]. In addition, while template cDNA was indeed amplified, each sample produced melt curves with two peaks, indicative of the presence of primer dimers [Figure 11B].

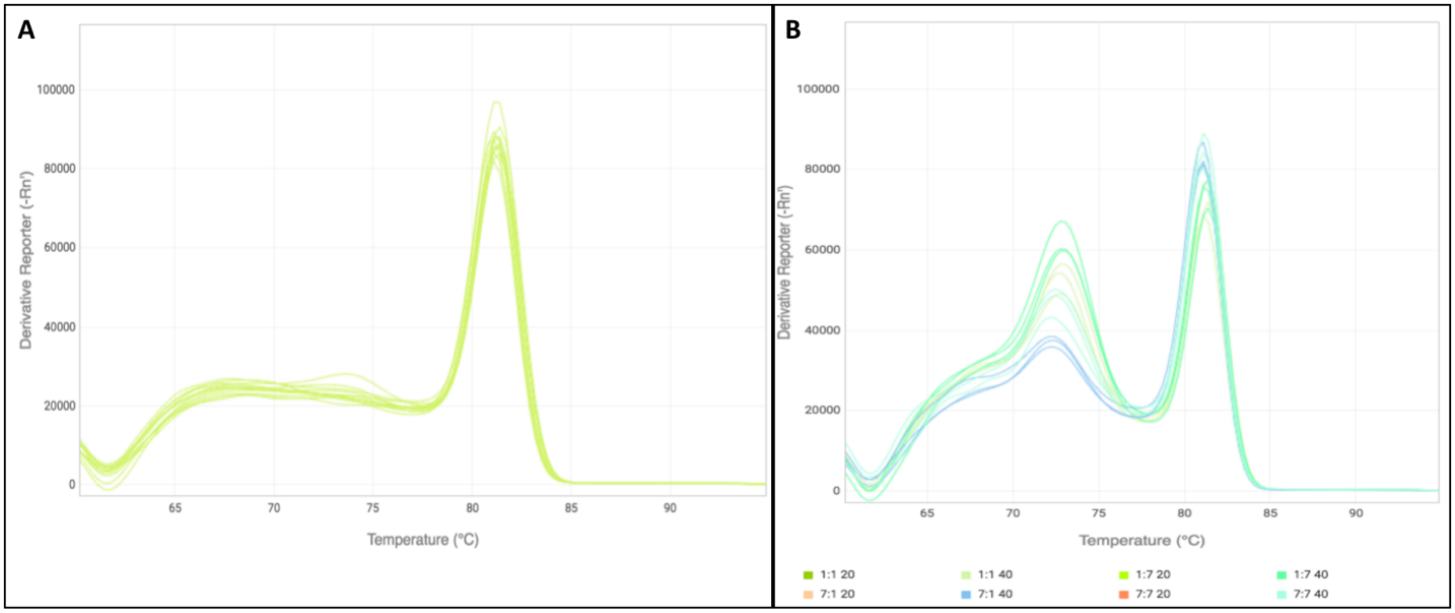

Figure 11. Melt curves generated from qPCR using ß-actin primers (various concentrations) and cDNA from brown anole brain tissue show contamination of NTC and substantial primer dimerization in template-containing reactions. Two-step RT-qPCR was performed to amplify the ß-actin gene. A) All NTCs had a large peak around 81ºC in the melt curve of each replicate. B) All cDNA-containing reactions has amplification of two products (81ºC and 75ºC), with the 7:1 primer ratio (dark blue) producing the least amount of the second product. In the graph legend, "20" represents use of 1:20 cDNA dilution and "40"represents 1:40 cDNA. Primer ratios are represented as 1:1, 1:7, 7:1, or 7:7 in graph legend.

B-actin is a highly conserved gene and therefore amplification of gDNA may seem like a reasonable cause of contamination, but the b-actin primers were confirmed to cross exon-exon boundaries of the target gene, so they should not have been able to bind nor amplify gDNA. Also, sterile conditions were used when preparing qPCR reactions so as to avoid contamination by any exogenous DNA. A more likely cause of contamination was template cDNA in one or more of the qPCR reagents that were used, including diluted primers, Power SYBR Green master mix, and/or sterile water.

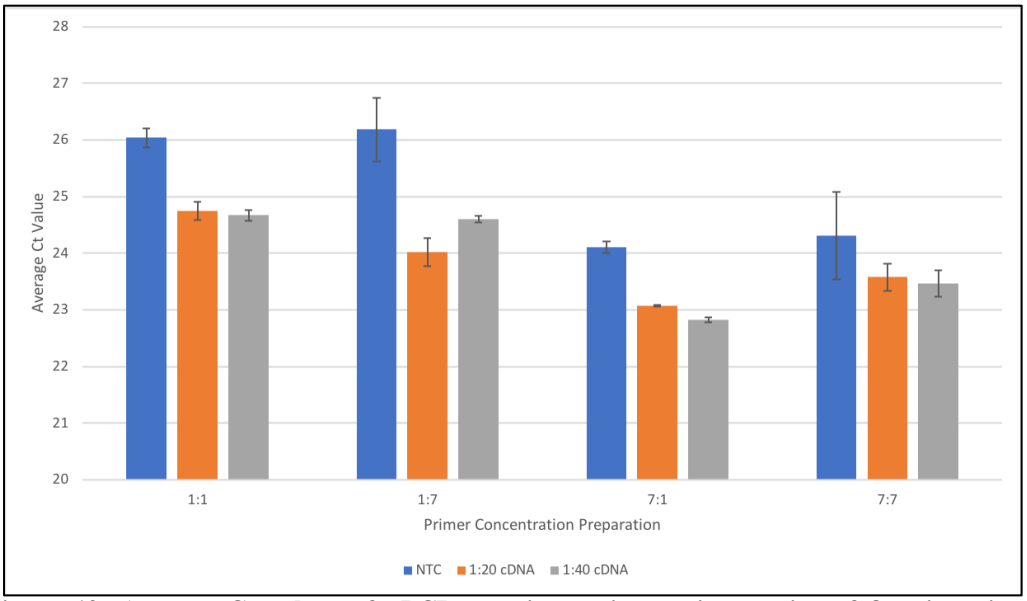

Figure 12. Average Ct values of qPCR reactions using various ratios of ß-actin primer concentrations and two cDNA dilutions (1:20 or 1:40) showed that a 1:1 ratio of forward: reverse primers yielded the highest Ct while a 7:7 ratio yielded the lowest. Each primer concentration ratio was tested in triplicate, using standard qPCR conditions, and the average is shown. Error bars represent standard deviation of each triplicate.

The second qPCR run for ß-actin tested 7:1, 8:1, and 9:1 ratios of forward: reverse primers, because the 7:1 ratio previously tested produced the best results in regards to low Ct values and lower incidences of primer dimers. Because there was still a significant presence of primer dimers in that sample, higher skews of primer ratios were tested to see if that could be improved. Clear peaks on the melt curves for the NTC indicated contamination, however, the 9:1 primer ratio NTC replicates showed much less amplification than 7:1 and 8:1 samples [Figure 13]. There is no true explanation for this, as all NTCs should have had complete lack of amplification, but it is evident that the NTC with 9:1 primer ratio somehow had much less than all other samples. This difference in contamination was not enough to consider this a successful qPCR run, though, as the average Ct value for each set of NTCs were still much too close to those of the cDNA-containing samples, clearly indicating contamination [Figure 14].

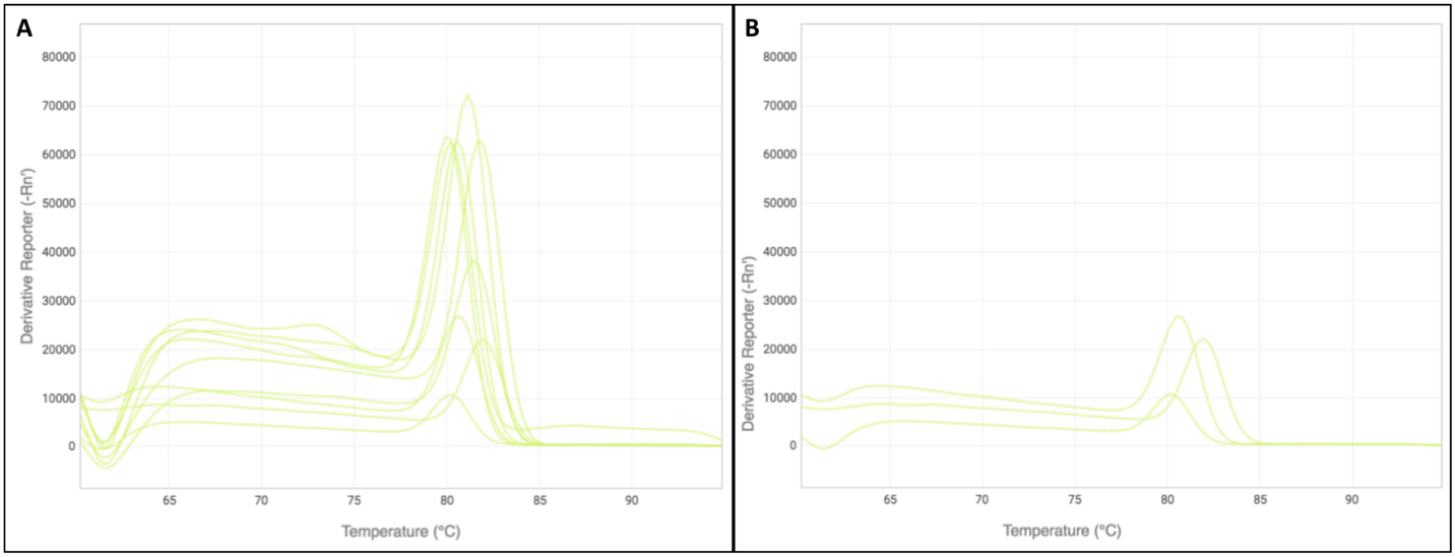

Figure 13. Melt curves generated from qPCR using ß-actin primers (various concentrations) and cDNA from brown anole brain tissue show contamination of NTC (A) with much less contamination in samples using a 9:1 primer ratio (B). Two-step RT-qPCR with standard conditions was used to amplify the ß-actin gene. A) All NTCs had a large peak around 81ºC in the melt curve of each replicate. B) The NTC replicates containing 9:1 ratio of primers had much smaller peaks around 81ºC on the melt curve.

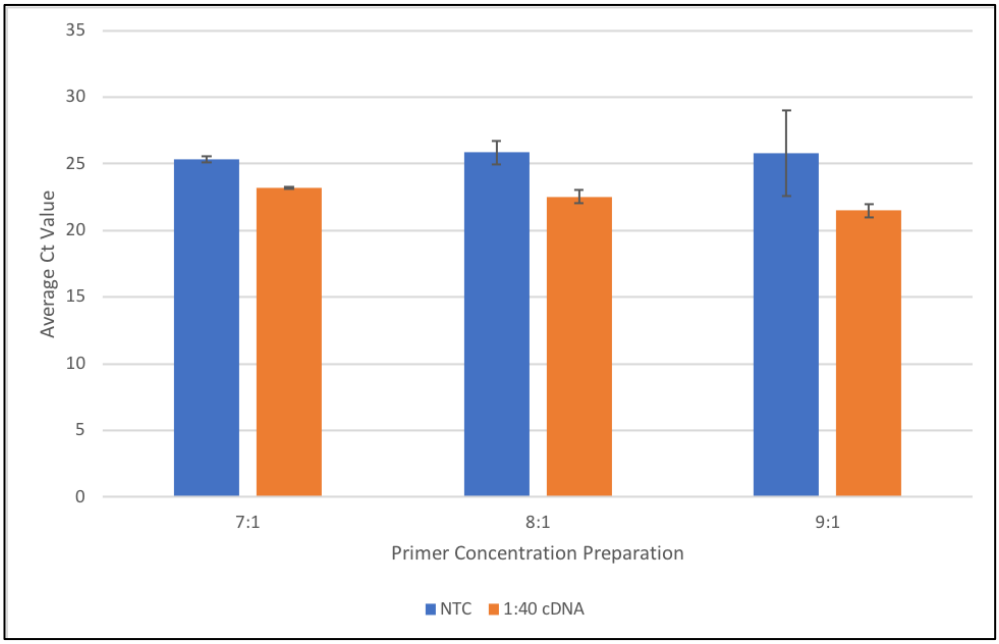

Figure 14. Average Ct values of qPCR reactions using various ratios of b-actin primer concentrations a cDNA dilution of 1:40 showed that primer concentrations skewed more than 7:1 did not affect average Ct value. Each primer concentration ratio was tested in triplicate, using standard qPCR conditions, and the average is shown. Error bars represent standard deviation of each triplicate.

Also, the 7:1 and 8:1 primer ratios still produced primer dimers in the samples containing cDNA template, as indicated by a second peak on the qPCR melt curves, but the 9:1 ratio produced mostly clean melt curves with a small second peak in one replication [Figure 15]. No clear optimal ratio of primer concentrations for b-actin were found, because 7:1, 8:1, and 9:1 primer ratios all produced roughly equal Ct values in both cDNA-containing samples and NTCs [Figure 14]. This inhibited future quantification of any target gene from the anole tissue samples, as ß-actin would be needed as an endogenous control for normalizing expression of all other genes.

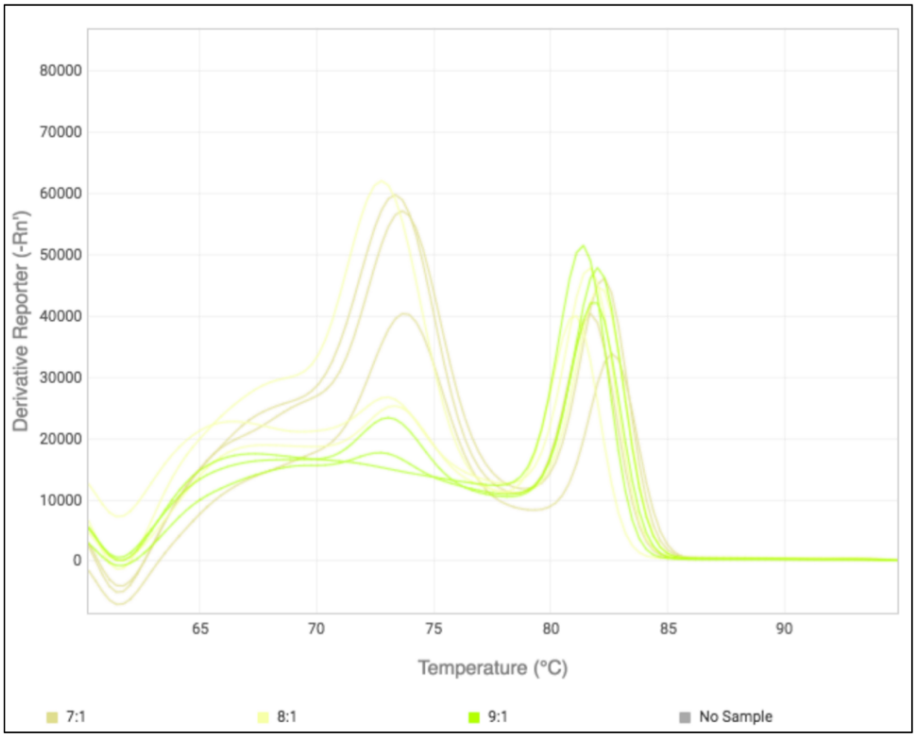

Figure 15. Melt curves generated from qPCR using b-actin primers (various concentrations) and cDNA from brown anole brain tissue show multiple products, indicating amplification of primer dimers. Two-step RT-qPCR with standard conditions was used to amplify the ß-actin gene. All cDNA-containing reactions has amplification of two products (81ºC and 74ºC). Primer ratios are represented as 7:1, 8:1, or 9:1 in graph legend.

Finally, a third qPCR run was done to test 1:1, 1:7, 7:1, and 7:7 primer ratios for CYP17a1 and StAR and also to troubleshoot the previous issue of NTC contamination. To eliminate all possible contamination in this qPCR step-up, new primer dilutions were made and new bottles of

master mix and water were used. This run was the most successful, with template-containing melt curves that almost all had a single clean peak and a nearly complete lack of contamination in NTCs [Figure 16].

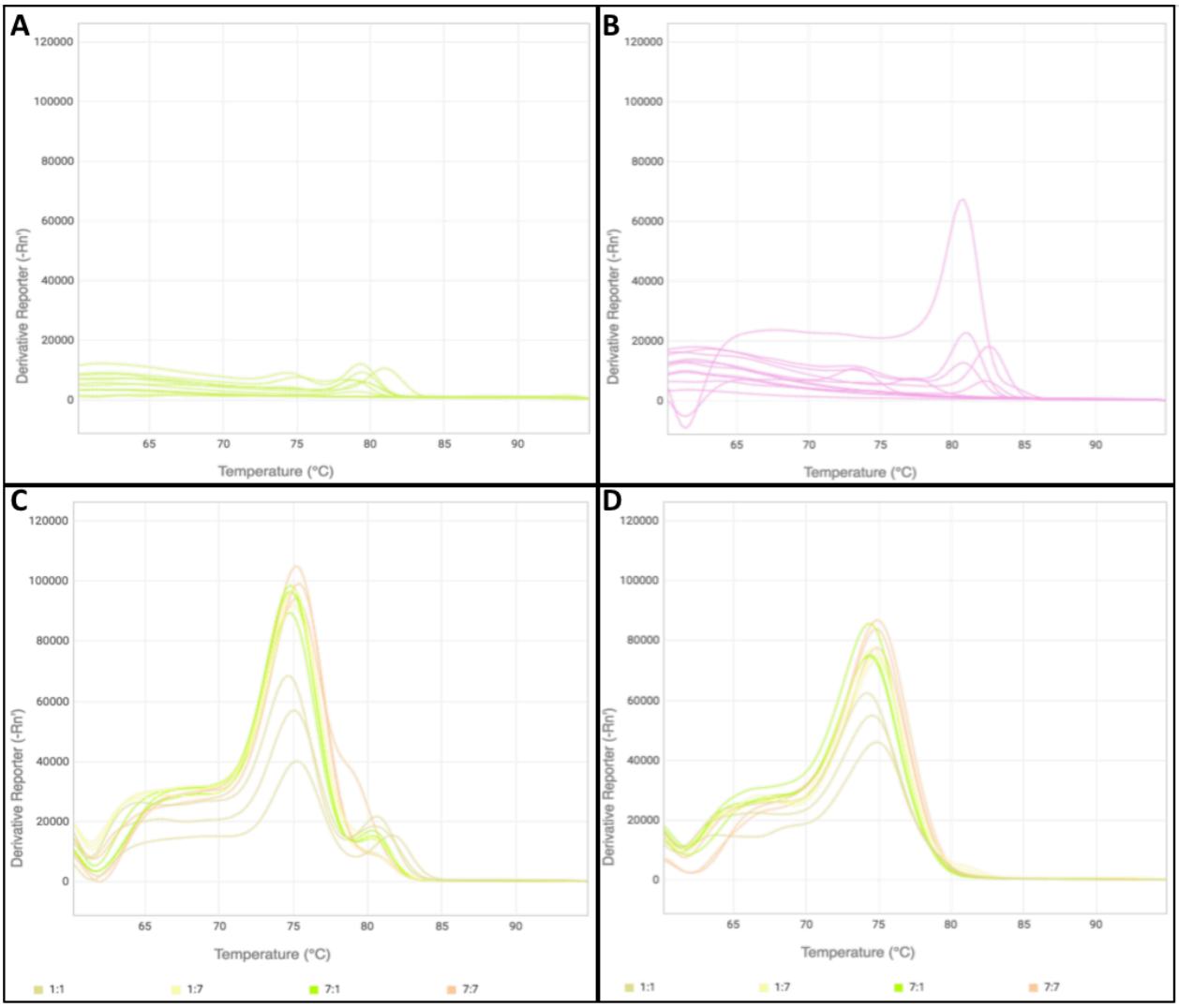

Figure 16. Melt curves generated from qPCR using CYP17a1 and StAR primers (various concentrations) with cDNA from brown anole brain tissue show no contamination of NTC (A and B) and little to no primer dimerization in template-containing reactions (C and D). Two-step RT-qPCR with standard conditions was used to amplify the CYP17a1 and StAR genes. A) CYP17a1 NTCs had flat peaks around 80ºC in the melt curves of each replicate. B) StAR NTCs had flat peaks around 80ºC in the melt curves of each replicate, aside from one replicate that showed a distinct peak. C) All CYP17a1 cDNA-containing reactions had a peak around 75ºC and a negligible second peak around 81ºC. D) All StAR cDNA-containing reactions had a peak around 75ºC. Primer ratios are represented as 1:1, 1:7, 7:1, or 7:7 in graph legends.

The extra precautions that were taken to achieve a sterile procedure seemed to be the necessary steps needed to eliminate NTC contamination, indicating that one or more of the qPCR reagents was contaminated with DNA. The primer concentration ratio that resulted in the lowest average Ct value for both CYP17a1 and StAR primers was 7:7 (17.5 µM of each primer) [Figure 17]. This was to be expected, as a higher availability of primers means that more template cDNA can be bound by primers and extended by DNA polymerase, leading to higher levels of replication at a faster pace, which ultimately allows the threshold level of amplification to be surpassed with fewer cycles. In future experiments that aim to quantify these genes, 17.5 µM of each primer can be used to maximize efficiency.

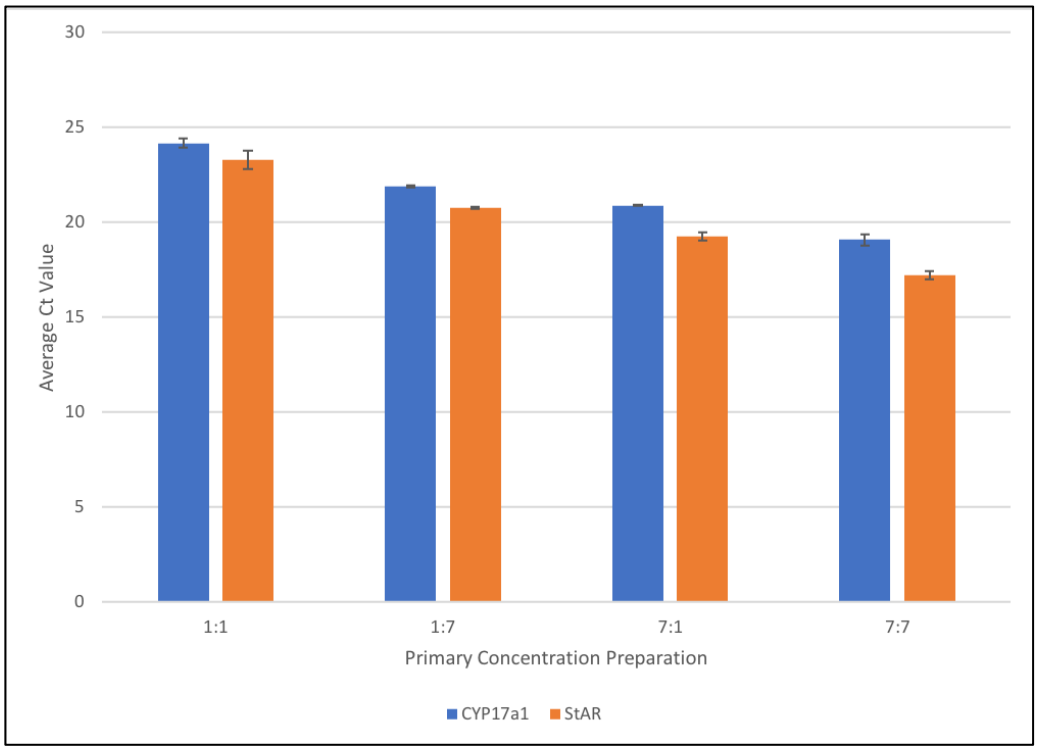

Figure 17. Average Ct values of qPCR reactions using various ratios of CYP17a1 and Star primer concentrations showed that a 1:1 ratio yielded the highest Ct while 7:7 yielded the lowest. Each primer concentration ratio was tested in triplicate, using standard qPCR conditions, and the average is shown. Error bars represent standard deviation of each triplicate.

After qPCR reactions were run, select samples were analyzed via gel electrophoresis to generally confirm amplification of the correct gene based on amplicon size. The next step to

definitively confirm target gene amplification would be to sequence the amplicons of each sample, but comparison of fragment sizes to expected size gives a good idea of the success of qPCR. Electrophoresis confirmed that ß-actin primers (7:1 ratio) amplified a fragment that was the same size as the expected amplicon (131 bp), as well as a smaller fragment that may represent primer dimers, and confirmed presence of contamination in the NTC [Figure 18].

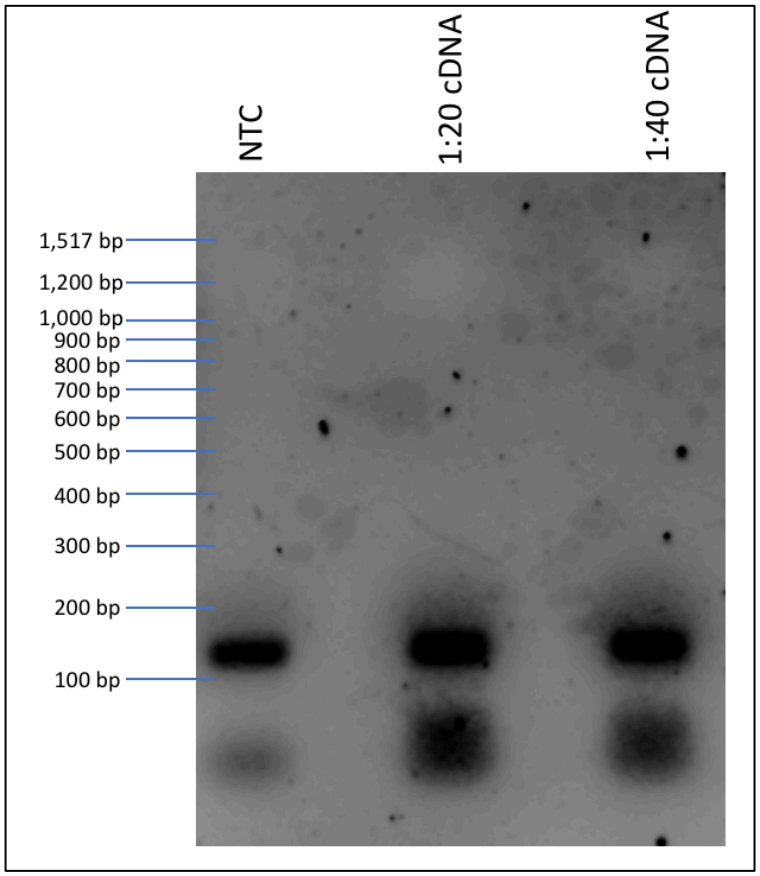

Figure 18. Samples from a qPCR run using -actin primers showed contamination of no-template control (NTC) and possibly successful amplification of ß-actin (with primer dimers) using both 1:20 and 1:40 dilutions of cDNA from brown anole brain tissue. Three qPCR reactions that used a 7:1 ratio of forward: reverse ß-actin primers were analyzed via standard gel electrophoresis (2% agarose in 1X TAE). The expected amplicon size of ß-actin is 131 bp.

Interestingly, although qPCR data analysis showed that a 9:1 primer ratio was best for lowering Ct values and primer-dimer formation in ß-actin samples, electrophoresis showed no clear 131 bp amplicon from any sample from the second qPCR run, including the 9:1 sample [Figure 19]. However, the expected amplicon was produced in the 7:1 and 8:1 NTCs, which should have had

no amplification [Figure 19]. This indicates significant contamination in these controls, which corresponds to qPCR data.

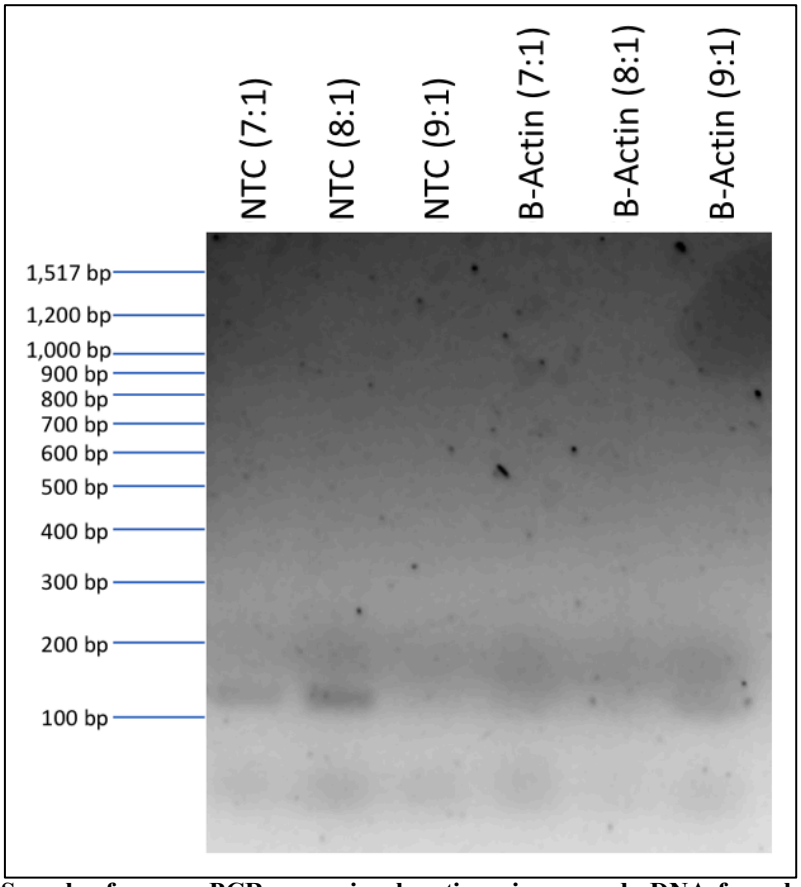

Figure 15. Samples from a qPCR run using b-actin primers and cDNA from brown anole brain tissue showed contamination of no-template control (NTC) and no successful amplification of ß-actin, regardless of primer concentration ratio. Six qPCR reactions that used a 7:1, 8:1, or 9:1 ratio of forward: reverse ß-actin primers were analyzed via standard gel electrophoresis (2% agarose in 1X TAE). The expected amplicon size of ß-actin is 131 bp.

Lastly, samples using CYP17a1 and StAR primers were also analyzed via gel electrophoresis. CYP17a1 primers produced amplicons of the expected size (86 bp) in each sample analyzed, except the NTCs, with the 7:7 primer ratio resulting in much more product than the 7:1 ratio [Figure 20]. This was to be expected, as higher concentrations of primers lead to higher rates of cDNA replication, as previously mentioned. Electrophoresis also showed that the qPCR set-up was done cleanly and that CYP17a1 primers did not have high rates of dimerization, as seen by no amplicons present in the NTC [Figure 20]. StAR primers, in contrast, did not produce amplicons

of the expected size (112 bp) when using 1:7 or 7:7 ratios, but did show faint presence of amplicons below 100 bp in all samples, including the NTC [Figure 20]. The amplicons from the reactions with template cDNA may have resulted from non-specific amplification of the template or amplification of primer dimers, with the latter being more like due to the specific nature of the StAR primers and the small size of the amplicons. Similarly, the amplicons produced in the NTCs are mostly likely primer dimers, due to their small size and the clean qPCR set-up that should not have allowed any template to be amplified in the NTC.

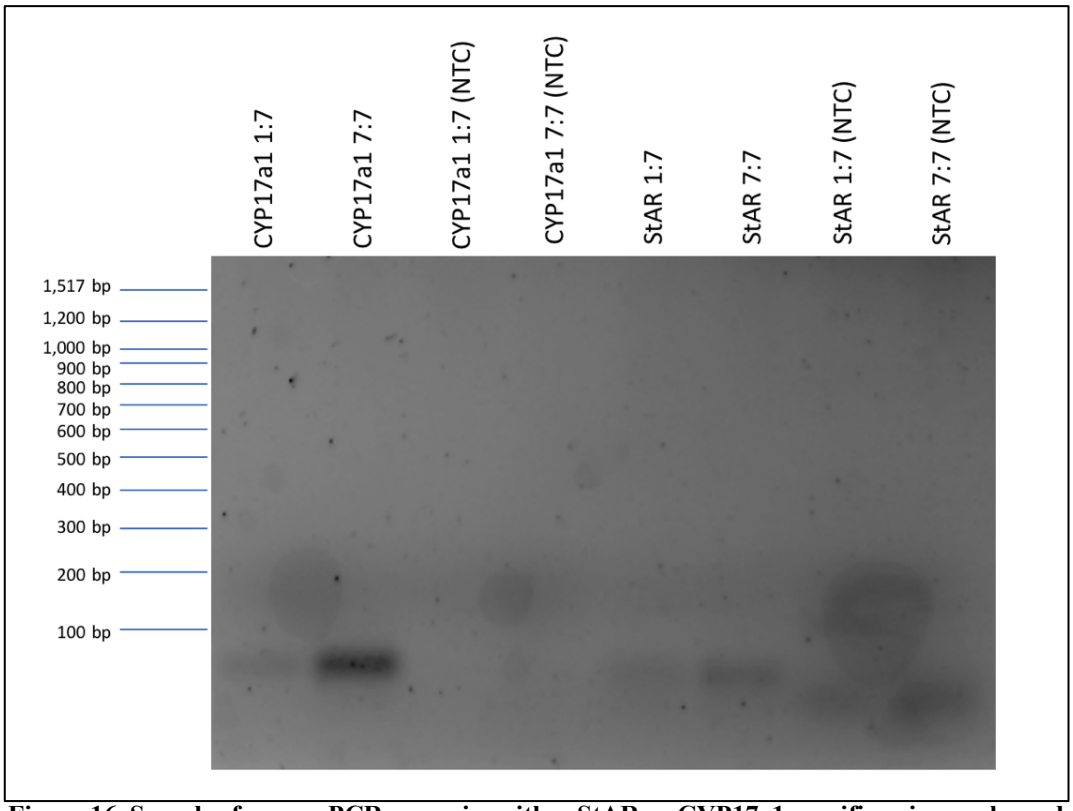

Figure 16. Samples from a qPCR run using either StAR or CYP17a1 specific primers showed potential amplification of the CYP17a1 gene, unsuccessful amplification of the StAR gene, and possible primer dimers in the StAR samples. Samples using either 1:7 or 7:7 forward: reverse primer concentration ratios were analyzed via standard agarose gel electrophoresis (2% agarose in 1X TAE). Expected amplicon size are 112 bp for StAR and 86 bp for CYP17a1.

Summary of Procedural Optimizations

Overall, this study included numerous validations and optimizations, but still did not achieve the goal of reliably quantifying steroidogenic gene expression in brown anole tissues for

comparison of fasted and fed anoles. The main improvement essential for future research in this species is primer design. While the primer sequences obtained from Peek (2017) met most of the necessary criteria, including being within 15-20 nucleotides, spanning exon-exon boundaries of mRNA, having no calculated dimerization abilities (with one exception), and having a G/C content between 30-80%, there is still room for improvement. The problem still remains of using primers to amplify genes from brown anole cDNA that were designed using the green anole genome. In the future, this problem could be overcome by designing and testing degenerate primers using the most conserved amino acid sequences of the target enzymes from multiple organisms related to the brown anole (Singh et al., 1998). Degenerate primers have variable bases, so that all the primers are slightly different and make up a library that covers the multiple sequence combinations that give rise to a single polypeptide sequence, which encodes for the target gene and is homologous among related organisms (Iserte et al., 2013). The set of degenerate primers can be tested via RT-PCR using RNA extracted from brown anole tissues, with green anole RNA as a positive control for primers with 100% homology to that organism. This method has been successfully used to amplify novel genes, including a surface antigen of hepatitis B virus (Singh et al., 1998). Therefore, this may be the best way to ensure specificity of primers with the unknown sequences of brown anole genes, allowing for clear and reliable quantification via qPCR in the future.

Aside from primers used in qPCR, another area for improvement is the RNA extraction procedure. This was optimized in the current study by reducing the amount of Trizol used and adding an extra centrifugation step to ensure separation of phenol and aqueous layers, as well as to ensure separation of tightly-bound proteins from RNA. However, a DNase step could be added at the end of the extractions to eliminate any traces of gDNA from being present in RNA samples that are ultimately used for quantification via qRT-PCR. Contamination of template RNA with

gDNA has been shown to cause false-positives during quantification and use of DNase on the same sample effectively eliminates that incorrect result (ThermoFisher Scientific, 2018). Presence of gDNA can be tested by using a no-RT control when reverse-transcribing extracted RNA into cDNA. Because RNA can only be converted into DNA via reverse-transcriptase, elimination of that enzyme should result in no cDNA synthesis in that sample. The no-RT control would then be analyzed via qPCR, along with experimental samples, and should have Ct values of five or more cycles below experimental samples, which indicates low or no presence of gDNA (Laurell et al., 2012).

Future Directions

By implementing all optimizations and suggested improvements discussed in this study, future research can be done to establish a connection between stress and local steroidogenesis in the brown anole via quantification of enzymatic gene expression. This would be novel information, as there is no published research clearly linking the two, nor is there even proof of local steroidogenesis via tissue-specific gene expression in this organism. The ideal tissue to begin with in the future is the brain, as the steroidogenic enzymes StAR and CYP19a1 have been discovered to be expressed here in some vertebrates (King et al., 2004). Also, RNA extracted from brain tissue was used in most of the optimizations in this study, showing its ability to yield pure RNA that is suitable for use in qRT-PCR.

Future studies using the RNA extraction and quantification optimizations established in this experiment could shed light onto the mechanisms of local hormonal regulation of stress and the next step could be to identify mRNA of steroidogenic enzymes in exosomes. Exosomes are small membrane-bound vesicles that are released from cells and serve as a form of intercellular communication (van Niel et al., 2006). Exosome release was first found to expel unwanted proteins

from cells, but later discovery of the ability of exosomes to bind to recipient cells opened many new possible functions of the vesicles (Raposo et al., 1996). It is suggested that exosomes can provided cell to cell communication via the delivery of RNA either within a microenvironment or at greater distances via circulation of exosomes in the blood stream (Valadi et al., 2007). While this has been studied in immune and tumor cells, the exchange of genetic information in steroidogenic cells has yet to be clearly and repeatedly established. Given the discovery of steroidogenic enzyme expression in local organ tissues, it is hypothesized that exosomes could serve as the vehicle for the mRNA that codes for these proteins, in addition to the utilization of local transcription to increase expression. To test this, exosomes could be isolated from brown anole tissue via serial microfiltration and centrifugation as previously done in Valadi et al. (2007). RNA would then be isolated from the exosomes and assessed via qRT-PCR to determine if genes for steroidogenic enzymes are present in the vesicles and in what quantity. Exosomes from tumor cells have been found to sometimes contain the steroidogenic enzyme CYP17A1, though it is not clear whether or not this is to promote androgen production in the recipient cells (Locke et al., 2009). Discovery of local steroidogenesis via exosomal mRNA exchange could provide a mechanism of tissue-specific steroid production that does not require local transcription, which would make the process much quicker and improve the efficiency of a systematic stress response.

In conclusion, the findings and optimizations performed in this study will beneficially impact future research on local steroidogenesis, potentially leading to verifications of the mechanisms of tissue-specific enzyme production. Improvements in primer design, via use of degenerate primers, and optimizations of primer concentrations for use in qRT-PCR, as laid out by the current study, would assist in studying the effects of fasting on local steroid synthesis in brown anoles, as well as the mechanisms that may alter those effects, such as exosomal mRNA

delivery. Research on this topic could pave the path for local steroidogenesis studies in humans, which could have clinical implications. The skin, for example, is a site for local steroidogenesis in mice (and possibly humans) and manipulation of this process could produce endogenous steroids that treat inflammation and immune malfunctions that are caused by disease (Slominski et al., 2013). Experiments in the brown anole that use the discoveries from our study could determine methods of therapeutic delivery of steroidogenic genes to tissues affected by disease, and overall can assist in novel discoveries related to local steroidogenesis.

References

Alföldi, J., Di Palma, F., Grabherr, M., Williams, C., Kong, L., Mauceli, E., Russell, P., Lowe, C.B., Glor, R.E., Jaffe, J.D., et al. (2011). The genome of the green anole lizard and a comparative analysis with birds and mammals. Nature *477*.

Altschul, S. F., Gish, W., Miller, W., Myers, E. W., and Lipman, D. J. (1990). Basic local alignment search tool. J. Mol. Biol. *215(3)*, 403-410.

Aranda, P.S., Lajoie, D.M., and Jorcyk, C.L. (2012). Bleach Gel: A Simple Agarose Gel for Analyzing RNA Quality. Electrophoresis *33*, 366–369.

De Boer, S.F., Koopmans, S., Slangen, J.L., and van der Gugten, J. (1989). Effects of fasting on plasma catecholamine, corticosterone and glucose concentrations under basal and stress conditions in individual rats. Physiol. Behav. *45*, 989–994.

Brindley, D.N., and Rolland, Y. (1989). Possible connections between stress, diabetes, obesity, hypertension and altered lipoprotein metabolism that may result in atherosclerosis. Clin. Sci. (Lond). *77*, 453–461.

Caraguel, C.G.B., Stryhn, H., Gagné, N., Dohoo, I.R., and Hammell, K.L. (2011). Selection of a Cutoff Value for Real-Time Polymerase Chain Reaction Results to Fit a Diagnostic Purpose: Analytical and Epidemiologic Approaches. J. Vet. Diagnostic Investig. *23*, 2–15.

Caron, K.M., Soo, S.-C., Wetsel, W.C., Stocco, D.M., Clark, B.J., Parker, K.L., and Estabrook, R.W. (1997). Targeted disruption of the mouse gene encoding steroidogenic acute regulatory protein provides insights into congenital lipoid adrenal hyperplasia. Med. Sci. *94*, 11540–11545.

Carvalhais, V., Delgado-Rastrollo, M., Melo, L.D.R., and Cerca, N. (2013). Controlled RNA contamination and degradation and its impact on qPCR gene expression in S. epidermidis biofilms. J. Microbiol. Methods *95*, 195–200.

Charmandari, E., Tsigos, C., and Chrousos, G. (2005). Endocrinology of the Stress Response. Annu. Rev. Physiol. *67*, 259–284.

Cizdziel, P.E., and Chomczynski, P. (1996). TRIzol: A New Reagent for Optimal Single-Step Isolation of RNA. Focus (Madison). *15*, 99–102.

Coumailleau, P., Kah, O., and Coumailleau, P. (2014). Cyp19a1 (Aromatase) Expression in the Xenopus Brain at Different Developmental Stages. J. Neuroendocrinol. *26*, 226–236.

Curnow, K.M., Tusie-Luna, M.-T., Pascoe, L., Natarajan, R., Gu, J.-L., Nadler, J.L., and White, P.C. (1991). The Product of the CYP11B2 Gene Is Required for Aldosterone Biosynthesis in the Human Adrenal Cortex. Mol. Endocrinol. *5*, 1513–1522.

DeFronzo, R.A., Sherwin, R.S., and Felig, P. (1980). Synergistic interactions of counterregulatory hormones: a mechanism for stress hyperglycemia. Acta Chir. Scand. Suppl. *498*, 33–42.

Desjardins, P., and Conklin, D. (2010). NanoDrop microvolume quantitation of nucleic acids. J. Vis. Exp.

Durkee, T.J., McLean, M.P., Hales, D.B., Payne, A.H., Waterman, M.R., Khan, I., and Gibori, G. (1992). P450(17 alpha) and P450SCC gene expression and regulation in the rat placenta. Endocrinology *130*, 1309–1317.

Feldmana, S., and Weidenfeldb, J. (1999). Glucocorticoid receptor antagonists in the hippocampus modify the negative feedback following neural stimuli. Brain Res. *821*, 33–37.

Gayral, P., Weinert, L., Chiari, Y., Tsagkogeorga, G., Ballenghien, M., and Altier, N.G. (2011). Next-generation sequencing of transcriptomes: a guide to RNA isolation in nonmodel

animals. Molec Eco Res *11*, 650–661.
Greenberg, N., Chen, T., and Crews, D. (1984). Social status, gonadal state, and the adrenal stress response in the lizard, Anolis carolinensis. Horm. Behav. *18*, 1–11.
Guyer, C., and Savage, J.M. (1986). Society of Systematic Biologists Cladistic Relationships Among Anoles (Sauria: Iguanidae) Cladistic Relationships among Anoles (Sauria: Iguanidae). Syst. Zool. *35,* 509-531.
Hales, D.B., and Payne, A.H. (1989). Glucocorticoid-Mediated Repression of P450scc mRNA de Novo Synthesis in Cultured Leydig Cells. Endocrinology *124*, 2099–2104.
Hawkins, C.L., and Davies, M.J. (1998). Hypochlorite-induced damage to proteins: formation of nitrogen-centred radicals from lysine residues and their role in protein fragmentation. Biochem J. *332*, 617–625.
Henley, D. V., Lindzey, J., and Korach, K.S. (2005). Steroid Hormones. In Endocrinology, (Totowa, NJ: Humana Press), pp. 49–65.
Herman, J.P., Ostrander, M.M., Mueller, N.K., and Figueiredo, H. (2005). Limbic system mechanisms of stress regulation: Hypothalamo-pituitary-adrenocortical axis. Prog. Neuro-Psychopharmacology Biol. Psychiatry *29*, 1201–1213.
Holzbauer, M., and Newport, H.M. (1967). The Effect of Stress on the Concentration of 3P-Hydroxypregn-5-en-20-one (Pregnenolone) and Pregn-4-ene-3,20-dione (Progesterone) in the Adrenal Gland of the Rat. *193*, 131–140.
Iserte, J.A., Stephan, B.I., Goñi, S.E., Borio, C.S., Ghiringhelli, P.D., and Lozano, M.E. (2013). Family-specific degenerate primer design: a tool to design consensus degenerated oligonucleotides. Biotechnol. Res. Int. *2013*, 383646.
Jacobson, L., and Sapolsky, R. (1991). The Role of the Hippocampus in Feedback Regulation of the Hypothalamic-Pituitary-Adrenocortical Axis. Endocr. Rev. *12*, 118–134.
Jankord, R., and Herman, J.P. (2008). Limbic Regulation of Hypothalamo-Pituitary-Adrenocortical Function during Acute and Chronic Stress. Ann N Y Acad Sci. *1148*, 64-73.
Joëls, M. (2009). Stress, the hippocampus, and epilepsy. Epilepsia *50*, 586–597.
Karishma, K.K., and Herbert, J. (2002). Dehydroepiandrosterone (DHEA) stimulates neurogenesis in the hippocampus of the rat, promotes survival of newly formed neurons and prevents corticosterone-induced suppression. Eur. J. Neurosci. *16*, 445–453.
Kang, K., Zhang, X., Liu, H., Wang, Z., Zhong, J., Huang, Z., Peng, X., Zeng, Y., Wang, Y., Yang, Y., et al. (2012). A Novel Real-Time PCR Assay of microRNAs Using S-Poly(T), a Specific Oligo(dT) Reverse Transcription Primer with Excellent Sensitivity and Specificity. PLoS One *7*, e48536.
Karishma, K.K., and Herbert, J. (2002). Dehydroepiandrosterone (DHEA) stimulates neurogenesis in the hippocampus of the rat, promotes survival of newly formed neurons and prevents corticosterone-induced suppression. Eur. J. Neurosci. *16*, 445–453.
Kayes-Wandover, K.M., and White, P.C. (2000). Steroidogenic Enzyme Gene Expression in the Human Heart [1]. J. Clin. Endocrinol. Metab. *85*, 2519–2525.
Keller-Wood, M.E., and Dallmann, M.F. (1984). Corticosteroid Inhibition of ACTH Secretion. Endocr. Rev. *5*, 1–24.
King, S.R., Ginsberg, S.D., Ishii, T., Smith, R.G., Parker, K.L., and Lamb, D.J. (2004). The Steroidogenic Acute Regulatory Protein Is Expressed in Steroidogenic Cells of the Day-Old Brain. Endocrinology *145*, 4775–4780.
de Kloet, E.R., Fitzsimons, C.P., Datson, N.A., Meijer, O.C., and Vreugdenhil, E. (2009).

Glucocorticoid signaling and stress-related limbic susceptibility pathway: About receptors, transcription machinery and microRNA. Brain Res. *1293*, 129–141.
Korade, Z., and Kenworthy, A.K. (2008). Lipid rafts, cholesterol, and the brain. Neuropharmacology *55*, 1265–1273.
Labrie, F., Luu-The, V., Bélanger, A., Lin, S.-X., Simard, J., Pelletier, G., and Labrie, C. (2005). Is dehydroepiandrosterone a hormone? J. Endocrinol. *187*, 169–196.
Laurell, H., Iacovoni, J.S., Abot, A., Svec, D., Maoret, J.-J., Arnal, J.-F., and Kubista, M. (2012). Correction of RT–qPCR data for genomic DNA-derived signals with ValidPrime. Nucleic Acids Res. *40*, e51–e51.
Leshner, A.I. (1980). The Interaction of Experience and Neuroendocrine Factors in Determining Behavioral Adaptations to Aggression. In Progress in Brain Research, pp. 427–438.
Leung, K., and Munck, A. (1975). Peripheral Actions of Glucocorticoids. Annu. Rev. Physiol. *37*, 245–272.
Locke, J. A., Nelson, C. C., Adomat, H. H., Hendy, S. C., Gleave, M. E., and Guns, E. S. (2009). Steroidogenesis inhibitors alter but do not eliminate androgen synthesis mechanisms during progression to castration-resistance in LNCaP prostate xenografts. J Steroid Biochem Mol Biol. 115(3-5), 126-136.
Losos, J. Brown and Green Anoles Dewlap Duetting. [Internet]. 2014 Jul 12. [cited 2017 Nov 20]. Anole Annals. Available from http://www.anoleannals.org/2014/07/12/brown-and-green-anoles-dewlap-duetting/
Malhotra, K., Foltz, L., Mahoney, W.C., and Schueler, P.A. (1998). Interaction and effect of annealing temperature on primers used in differential display RT-PCR. Nucleic Acids Res. *26*, 854–856.
Manthey, J.D., Tollis, M., Lemmon, A.R., Moriarty Lemmon, E., and Boissinot, S. (2016). Diversification in wild populations of the model organism *Anolis carolinensis* : A genome-wide phylogeographic investigation. Ecol. Evol. *6*, 8115-8125.
McEwen, B.S., Weiss, J.M., and Schwartz, L.S. (1968). Selective Retention of Corticosterone by Limbic Structures in Rat Brain. Nature *220*, 911–912.
McGillis, J.P., Park, A., Rubin-Fletter, P., Turck, C., Dallman, M.F., and Payan, D.G. (1989). Stimulation of rat B-lymphocyte proliferation by corticotropin-releasing factor. J. Neurosci. Res. *23*, 346–352.
Mikeska, T., Dobrovic, A., and Dobrovic -AlexanderDobrovic, A. (2009). Validation of a primer optimisation matrix to improve the performance of reverse transcription – quantitative real-time PCR assays. BMC Res. Notes *2*, 1–5.
Miller, W. (2013). A brief history of adrenal research Steroidogenesis- The soul of the adrenal gland. Mol Cell Endo *371*, 5–14.
Miller, W.L. (1988). Molecular Biology of Steroid Hormone Synthesis. Endocr. Rev. *9*, 295–318.
Mindnich, R., Möller, G., and Adamski, J. (2004). The role of 17 beta-hydroxysteroid dehydrogenases. Mol. Cell. Endocrinol. *218*, 7–20.
Morsink, M.C., Steenbergen, P.J., Vos, J.B., Karst, H., Joels, M., Kloet, E.R., and Datson, N.A. (2006). Acute Activation of Hippocampal Glucocorticoid Receptors Results in Different Waves of Gene Expression Throughout Time. J. Neuroendocrinol. *18*, 239–252.
Muller, C., Hennebert, O., and Morfin, R. (2006). The native anti-glucocorticoid paradigm. J. Steroid Biochem. Mol. Biol. *100*, 95–105.
Munck, A., Guyre, P.M., and Holbrook, N.J. (1984). Physiological Functions of Glucocorticoids in Stress and Their Relation to Pharmacological Actions. Endocr. Rev. *5*, 25–44.

van Niel, G., Porto-Carreiro, I., Simoes, S., and Raposo, G. (2006). Exosomes: A Common Pathway for a Specialized Function. J. Biochem. *140*, 13–21.

O'Shaughnessy, P.J., Willerton, L., and Baker, P.J. (2002). Changes in Leydig cell gene expression during development in the mouse. Biol. Reprod. *66*, 966–975.

Oberbeck, R., Benschop, R.J., Jacobs, R., Hosch, W., Jetschmann, J.U., Schürmeyer, T.H., Schmidt, R.E., and Schedlowski, M. (1998). Endocrine mechanisms of stress-induced DHEA-secretion. J. Endocrinol. Invest. *21*, 148–153.

Parker, C.R., Stankovic, A.M., and Goland, R.S. (1999). Corticotropin-releasing hormone stimulates steroidogenesis in cultured human adrenal cells. Mol. Cell. Endocrinol. *155*, 19–25.

Parker, K.L., Chaplin, D.D., Wong, M., Seidman, J.G., Smith, J.A., and Schimmer, B.P. (1985). Expression of murine 21-hydroxylase in mouse adrenal glands and in transfected Y1 adrenocortical tumor cells. Proc. Natl. Acad. Sci. USA *82*, 7860–7864.

Payne, A.H., and Hales, D.B. Overview of Steroidogenic Enzymes in the Pathway from Cholesterol to Active Steroid Hormones. Endocr Reviews. *25(6)*, 947-970.

Peek, C. (2017). Steroidogenesis in the Green Anole Lizard Brain and Gonad. Minnesota State University: All Theses, Dissertations, and Other Capstone Projects. 736.

Penning, T.M. (1997). Molecular Endocrinology of Hydroxysteroid Dehydrogenases. Endocr. Rev. *18*, 281–305.

Raposo, G., Nijman, H.W., Stoorvogel, W., Liejendekker, R., Harding, C. V, Melief, C.J., and Geuze, H.J. (1996). B lymphocytes secrete antigen-presenting vesicles. J. Exp. Med. *183*, 1161–1172.

Ririe, K.M., Rasmussen, R.P., and Wittwer, C.T. (1997). Product Differentiation by Analysis of DNA Melting Curves during the Polymerase Chain Reaction. Anal. Biochem. *245*, 154–160.

Ririe, K.M., Rasmussen, R.P., and Wittwer, C.T. (1997). Product Differentiation by Analysis of DNA Melting Curves during the Polymerase Chain Reaction. Anal. Biochem. *245*, 154–160.

Sanderson, J.T. (2006). The Steroid Hormone Biosynthesis Pathway as a Target for Endocrine-Disrupting Chemicals. Tox Sci *94*, 3–21.

Sapolsky, R.M., Romero, L.M., and Munck, A.U. (2000). How Do Glucocorticoids Influence Stress Responses? Integrating Permissive, Suppressive, Stimulatory, and Preparative Actions [1]. Endocr. Rev. *21*, 55–89.

Sawada, H., Ibi, M., Kihara, T., Urushitani, M., Akaike, A., and Shimohama, S. (1998). Estradiol protects mesencephalic dopaminergic neurons from oxidative stress-induced neuronal death. J. Neurosci. Res. *54*, 707–719.

Sawchenko, P.E. (1987). Adrenalectomy-induced enhancement of CRF and vasopressin immunoreactivity in parvocellular neurosecretory neurons: anatomic, peptide, and steroid specificity. J. Neurosci. *7*, 1093–1106.

Silverin, B., Baillien, M., and Balthazart, J. (2004). Territorial aggression, circulating levels of testosterone, and brain aromatase activity in free-living pied flycatchers. Horm. Behav. *45*, 225–234.

Simpson, E.R., Clyne, C., Rubin, G., Boon, W.C., Robertson, K., Britt, K., Speed, C., and Jones, M. (2002). Aromatase—A Brief Overview. Annu. Rev. Physiol. *64*, 93–127.

Singh, V.K., Mangalm, A.K., Dwivedi, S., and Naik, S. (1998). Primer premier: program for design of degenerate primers from a protein sequence. BioTech *24*, 318–319.

Slominski, A., Zbytek, B., Nikolakis, G., Manna, P.R., Skobowiat, C., Zmijewski, M., Li, W., Janjetovic, Z., Postlethwaite, A., Zouboulis, C.C., et al. (2013). Steroidogenesis in the skin: implications for local immune functions. J. Steroid Biochem. Mol. Biol. *137*, 107–123.

Smith, S.M., and Vale, W.W. (2006). The role of the hypothalamic-pituitary-adrenal axis in neuroendocrine responses to stress. Dialogues in Clin Neurosci. *8(4)*, 383-395.

Stocco, D.M. (2000). The role of the StAR protein in steroidogenesis: challenges for the future. J. Endocrinol. *164*, 247–253.

Taves, M.D., Gomez-Sanchez, C.E., and Soma, K.K. (2011). Extra-adrenal glucocorticoids and mineralocorticoids: evidence for local synthesis, regulation, and function. Am J Physiol Endocrinol Metab. *301*, E11-E24.

Thermo Fisher Scientific (2009). NanoDrop Spectrophotometers. T042 Tech. Bull. 1–2.

Thermo Fisher Scientific (2011). Power SYBR ® Green PCR Master Mix and Power SYBR ® Green RT-PCR Reagents Kit. User Guid. *4368577*.

Thermo Fisher Scientific (2018). RNA Isolation for qRT-PCR. Tech. Ref. Libr.

Tokarz, R. (1987). Effects of corticosterone treatment on male aggressive behavior in a lizard (Anolis sagrei). Horm. Behav. *21*, 358–370.

Tokarz, R.R., Mcmann, S., Seitz, L., and John-alder, H. (2017). Division of Comparative Physiology and Biochemistry, Society for Integrative and Comparative Biology Plasma Corticosterone and Testosterone Levels during the Annual Reproductive Cycle of Male Brown Anoles (Anolis sagrei). Source Physiol. Zool. *71*, 139–146.

Valadi, H., Ekström, K., Bossios, A., Sjöstrand, M., Lee, J.J., and Lötvall, J.O. (2007). Exosome-mediated transfer of mRNAs and microRNAs is a novel mechanism of genetic exchange between cells. Nat. Cell Biol. *9*, 654–659.

Watts, A.G. (2005). Glucocorticoid regulation of peptide genes in neuroendocrine CRH neurons: A complexity beyond negative feedback. Front. Neuroendocrinol. *26*, 109–130.

Ye, J., Coulouris, G., Zaretskaya, I., Cutcutache, I., Rozen, S., and Madden, T.L. (2012). Primer-BLAST: A tool to design target-specific primers for polymerase chain reaction. BMC Bioinformatics *13*, 1–11.